BNL-221795-2021-TECH
C-A/AP/646

Simulations of RHIC Spin Flipper

P. Adams

July 2021

Collider Accelerator Department
Brookhaven National Laboratory

U.S. Department of Energy
USDOE Office of Science (SC), Nuclear Physics (NP) (SC-26)

DISCLAIMER

Simulations of RHIC Spin Flipper

P. Adams, F. Méot, H. Huang, J. Kewisch, P. Oddo, T. Roser

Collider-Accelerator Department, BNL, Upton, NY 11973

July 7, 2021

Abstract

The extensive APEX studies of the RHIC Spin Flipper were performed during FY17 achieving up to 97 % spin flip efficiency at both injection (23.8 GeV) and store (255 GeV) energy, using 9 MHz and 197 MHz RF system. The Zgoubi simulations were setup to reproduce the experimental conditions. The results of the APEX measurements and the numerical simulations are compared here, showing a good agreement especially at injection energy. The additional simulations of the spin flip efficiency, with the 28 MHz and 197 MHz RF system, show that a stronger Spin Flipper is needed in order to achieve good ($|P_f/P_i| > 99$ %) spin flip efficiency during the nominal physics store running conditions at 255 GeV.

Tech. Note CA/AP/646
BNL C-AD

Contents

1 Spin Flipper

Spin physics programs in the Relativistic Heavy Ion Collider (RHIC) and in the future Electron Ion Collider (EIC) require a measurement of bunch polarization with great accuracy. The spin flipper was designed to reverse the polarization sign of all bunches during the stores without changing other beam parameters or machine settings, in order to reduce the systematic errors of the polarization measurements.

1.1 Design

The Spin Flipper (SF) consists of four horizontal dipoles ("spin rotator") and five vertical AC dipoles (Fig. 1) [1].

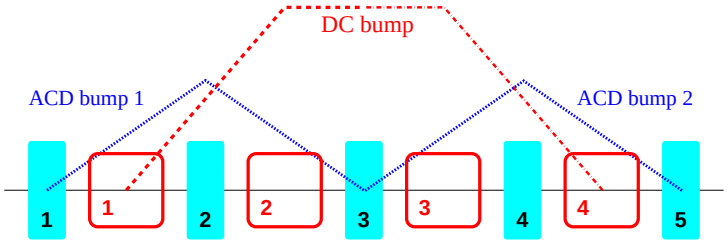

Figure 1: Spin Flipper layout

The four y-rotator dipoles (vertical field) are DC, with field integral $\mathrm{B_{dc}L}$. They yield spin rotation angles $+\psi_0/-\psi_0/-\psi_0/+\psi_0$ respectively, with

$$\psi_0 = (1+\mathrm{G}\gamma)\frac{\mathrm{B_{dc}L}}{\mathrm{B}\rho} \tag{1}$$

Orbit-wise this defines a closed local horizontal bump and, spin-wise, it leaves the spin tune $\nu_\mathrm{s} \approx 1/2$ unchanged.

The horizontal magnetic field in the AC dipoles has the form $\mathrm{B_{osc}(t)} = \hat{\mathrm{B}}_\mathrm{osc}\cos(2\pi \mathrm{f_{osc}(t)t} + \varphi_0)$ with $\mathrm{f_{osc}(t)}$ the time-varying oscillation frequency and φ_0 a reference phase. ACD1-3 and ACD3-5 triplets both ensure the same $+\phi_\mathrm{osc}(\mathrm{t})/-2\phi_\mathrm{osc}(\mathrm{t})/+\phi_\mathrm{osc}(\mathrm{t})$ spin x-rotation sequence, with

$$\phi_\mathrm{osc}(\mathrm{t}) = (1+\mathrm{G}\gamma)\frac{\mathrm{B_{osc}(t)L}}{\mathrm{B}\rho} \tag{2}$$

Orbit-wise, each triplet ensures a locally closed vertical orbit bump (Fig. 1). The phases of the first (ACD1-3) and second (ACD3-5) vertical bumps are correlated, namely,

$$\varphi_{0,\mathrm{ACD1-3}} - \varphi_{0,\mathrm{ACD3-5}} = \pi + \psi_0 \tag{3}$$

This configuration of the AC dipole assembly induces a spin resonance at $\nu_\mathrm{osc} = \nu_\mathrm{s}$, with the phase relationship (Eq. 3) canceling the image resonance at $(1-\nu_\mathrm{s})$. This allows for the spin tune to remain $\frac{1}{2}$ during the spin flip [2]).

1.2 Spin flip efficiency

Froissart-Stora formula describes the spin flip efficiency for the single resonance crossing,

$$\mathrm{P_f} = \mathrm{P_i}\left(2\exp^{-\frac{\pi}{2}\frac{|\epsilon|^2}{\alpha}} - 1\right) \tag{4}$$

where $\mathrm{P_i}$ and $\mathrm{P_f}$ is the initial and asymptotic polarization.
The strength of the spin resonance excitation is

$$|\epsilon| = \frac{\phi_{\mathrm{osc}}}{\pi} \sin\psi_0 \sin\frac{\psi_0}{2} \tag{5}$$

The crossing speed (rate of sweep of ν_{osc} through $\nu_{\mathrm{s}} \approx \frac{1}{2}$) is

$$\alpha = \frac{\Delta\nu_{\mathrm{osc}}}{\mathrm{d}\theta}, \quad \mathrm{d}\theta = 2\pi\mathrm{N} \tag{6}$$

with $\Delta\nu_{\mathrm{osc}}$ the AC dipole frequency span and N the number of turns of the sweep.
Sweep time is the period during which the AC dipole frequency is changing, $\tau_{\mathrm{X}} = \mathrm{NT_{rev}}$, where $\mathrm{T_{rev}}$ is the revolution period.

1.3 Spin tune oscillations and multiple resonance crossings

The synchrotron motion induces the spin tune ν_{s} oscillations [1] [3],

$$\delta\nu_{\mathrm{s}} = \frac{1+\mathrm{G}\gamma}{\pi}\Delta\mathrm{D}'\frac{\Delta\mathrm{p}}{\mathrm{p}} \tag{7}$$

where $\Delta\mathrm{D}'$ is a difference of the dispersion function derivatives at the two snakes. Since the AC dipole frequency is linearly swept across ν_{s} this effect can for large $\Delta\mathrm{D}'$ and small crossing speeds induce multiple crossing of the resonance, as demonstrated in Fig. 2, and thus cause the polarization loss during the spin flip.

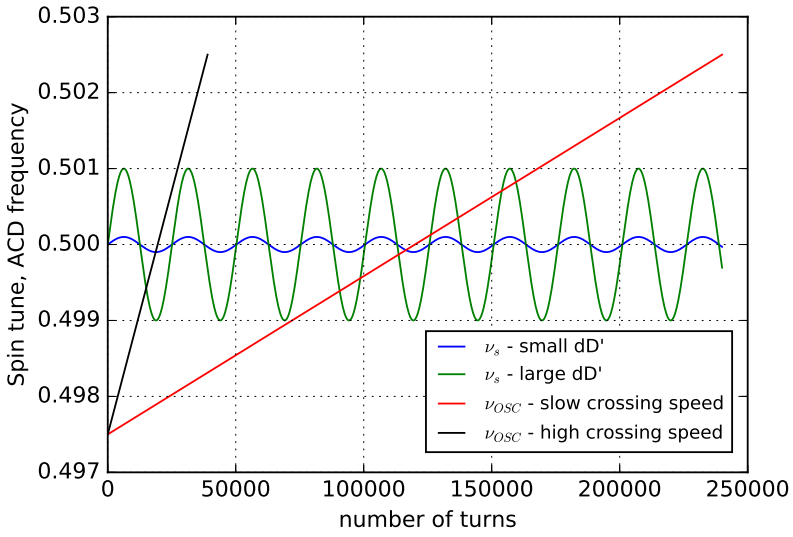

Figure 2: Spin tune oscillations cause multiple resonance crossings for large $\Delta D'$ and small crossing speed.

2 Experimental Setup during FY17 APEX Studies

The Spin Flipper APEX experiments were conducted over several dedicated periods during Run 17 [4]. Nominal RHIC lattice, betatron tunes, chromaticities, beam conditions and RF settings (dual harmonic 9MHz+197MHz; the 255 GeV measurements were done before re-bucketing) were used. The details are shown in Tab. 1. The Spin Flipper parameters are listed in Tab. 2. An example of the AC dipole up/down ramp is shown in Fig. 5. $\gamma_{\rm tr}$ quads were used to vary ΔD$'$ with marginal effect on RHIC optics. ΔD$'$ was scanned down from nominal 63 mrad to 3 mrad at 23.8 GeV and to 0.12 mrad at 255 GeV. The Siberian snake currents were 323 A and 100 A for most of the time.

Fig. 3 shows the measured beam orbit around the RHIC ring. At injection an IP10 horizontal bump ($\approx -25\mathrm{mm}$) needs to be inserted in order to be able to operate the Spin Flipper, since the horizontal bump created by DC dipoles is around +50mm inside the Spin Flipper at this energy. The DC bump is not visible on the orbit display since there are no BPMs within the Spin Flipper. Other orbit bumps such as the dump bump, vertical separation bumps and snake bumps were present during the injection measurements. At 255 GeV only the vertical separation bumps at IPs were on.

The Wall Current Monitor measurements of the longitudinal phase distribution at both injection and store energy (before re-bucketing) are shown in Fig. 4.

Table 1: RHIC optics, RF and bunch settings. The simulations were set up to closely reproduce APEX lattice, RF, and bunch properties. The indices 9 and 197 of the double-RF system voltages and synchronous phase and frequency refer to the 9.4 MHz and 197 MHz, respectively.

		injection	store
Energy	(GeV)	23.81	255
Gγ		45.5	487.0
Bρ	(T m)	79.37	850.6
Momentum compaction	(10^{-3})	1.95	1.92
Tunes $\nu_{\rm x}$; $\nu_{\rm y}$		28.695; 29.687	28..689; 29.684
Chromaticities $\xi_{\rm x}$; $\xi_{\rm y}$		5; 5	
$\beta^*_{\rm x}$; $\beta^*_{\rm y}$, at IP6	(m)	10; 10	1.4; 1.4
Double-RF system :			
$f_{\rm RF}$	(MHz)	9.4 & 197	
$f_{\rm RF}/f_{\rm rev}$		120 & 2520	
Voltages V_9; V_{197}	(kV)	22; 10	30; 15
Synch. phase ϕ_9	(rad)	π	
Synch. freq. $f_{\rm s} = \frac{\Omega_9}{2\pi}$	(Hz)	6.5	5.1
Bunch emittances, length, momentum spread:			
$\beta\gamma\varepsilon_{\rm x,y}$, *rms*	(μm)	2.5	
Length, *full*	(ns)	$\pm$15	
δp/p, *full*	(10^{-3})	$\pm$1.5	$\pm$0.25

Table 2: Spin flipper settings in the APEX.

		injection	store
Energy	(GeV)	23.8	255
$(1+\mathrm{G}\gamma)/\mathrm{B}\rho$	$(\mathrm{T\,m})^{-1}$	0.5859	0.5740
$\mathrm{B_{dc}L}$	(T m)	0.8905	1.4842
ψ_0 (Eq. 1)	(deg)	29.893	48.813
$\mathrm{B_{osc}L}$	(T m)	0.01	
ϕ_{osc} (Eq. 2)	(deg)	0.3357	0.3289
ϵ_{K} (Eq. 5)	(10^{-4})	2.396	5.679
ACD sweep parameters:			
$\Delta\nu_{\mathrm{osc}}$ range		0.005	
Sweep duration τ_{X}	(s)	0.5 - 3	
Up and down ramps	(s)	1.5	

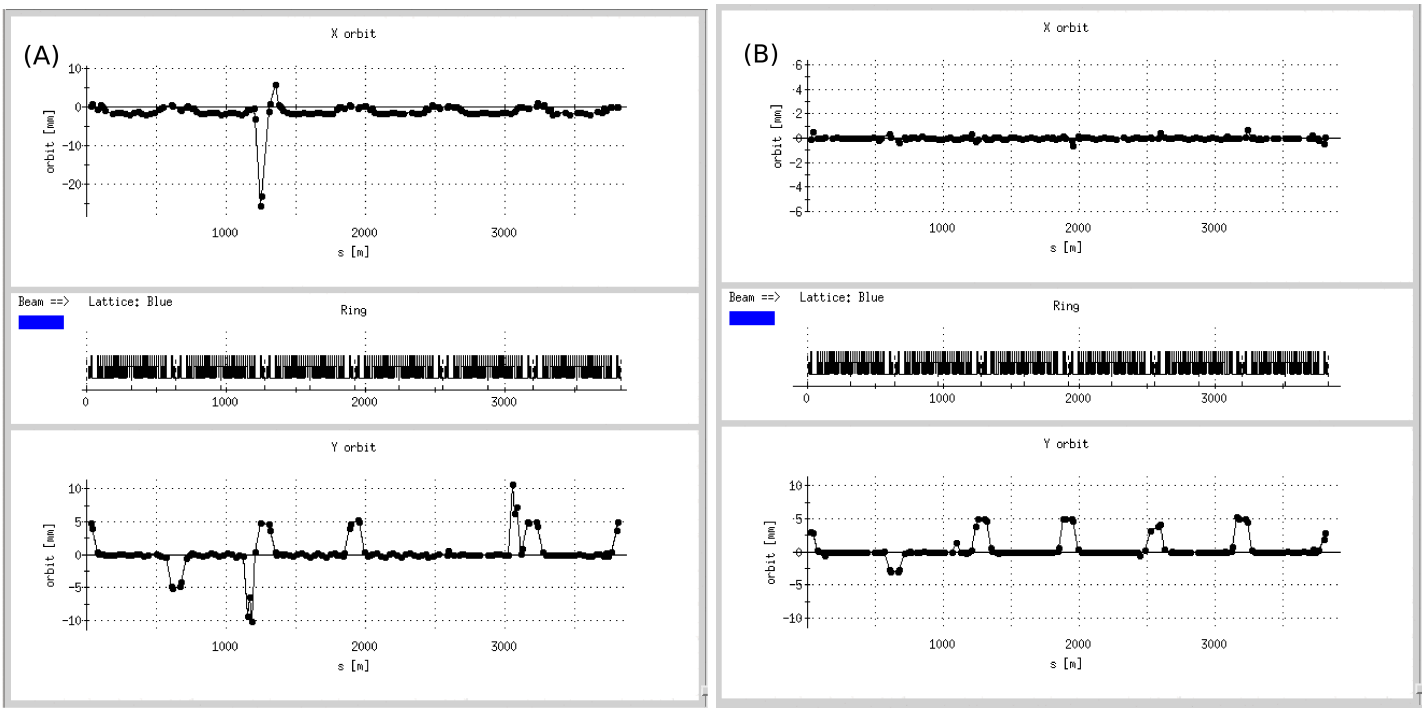

Figure 3: RHIC orbit: (A) at 23.8 GeV, (B) at 255 GeV.

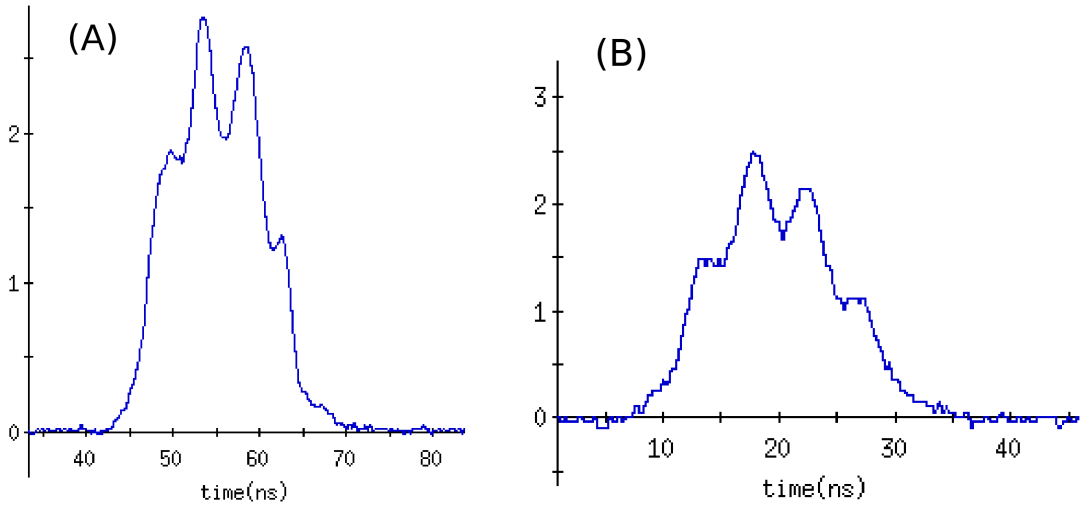

Figure 4: Wall current monitor data: (A) at 23.8 GeV, (B) at 255 GeV.

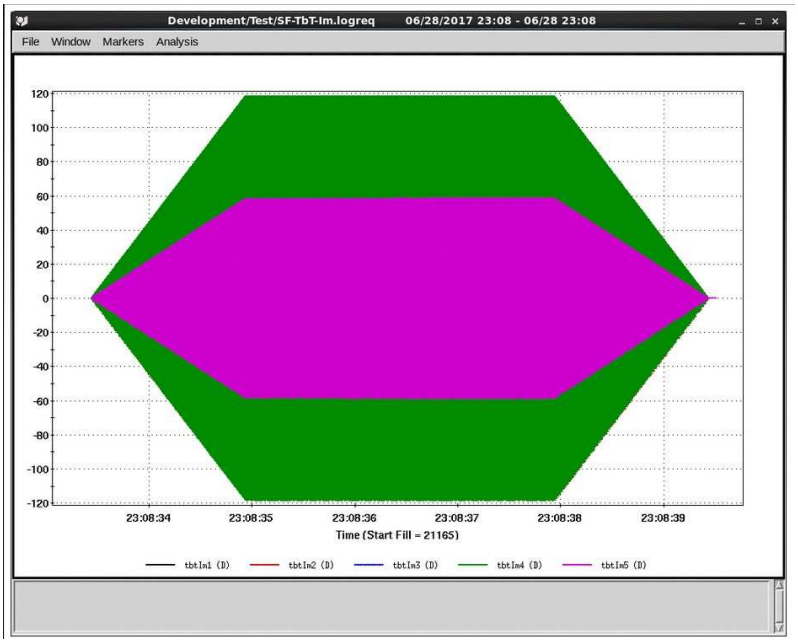

Figure 5: An example of the AC dipole function. The up/down ramps are 1.5 s long. The frequency sweep is 3 s long.

3 Zgoubi simulation setup

The Zgoubi input files were created using RHIC lattice MADX files with the start of the optical sequence at IP6. The spin flipper assembly was incorporated into the lattice as well as its ramping and frequency sweep. The betatron tunes, chromaticities and RF settings were adjusted to match the experimental conditions. The Siberian snakes were added only as pure spin rotators, using 'SPINR' keyword in Zgoubi code [5], by defining two angles: ϕ_Z an angle (in (X,Y) plane) between the X-axis and the spin precession axis; μ spin precession angle around this axis; ϕ_Z was used to fine-adjust the spin tune.

3.1 Orbit

Most of the simulations were done without RHIC orbit bumps. The separation bump at IP10 causes the stable spin direction to be vertically tilted at the spin flipper location as demonstrated in Fig. 6. Its presence has no effect on the spin flip efficiency if the Spin Flipper is well balanced, as shown in Tab. 7. The Spin Flipper orbit bumps are plotted in Fig. 7 to point out the presence and the strength of the AC (at full amplitude) and DC dipoles.

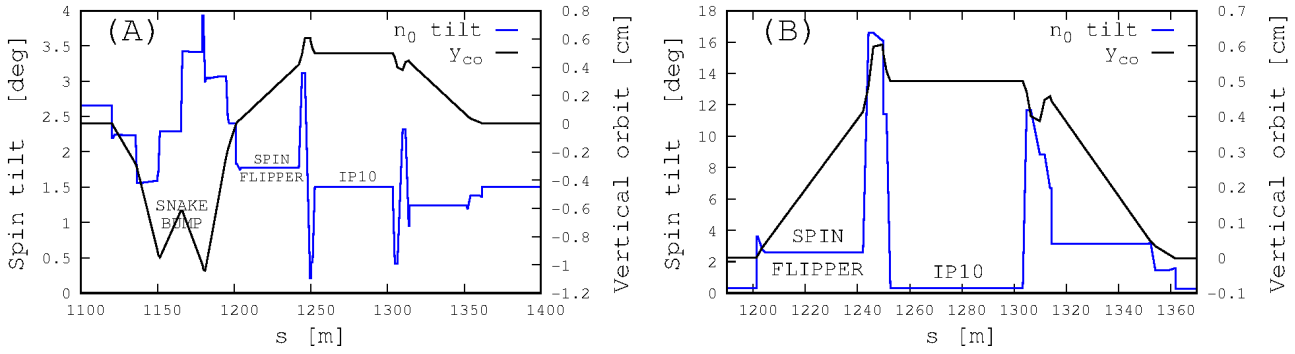

Figure 6: The spin flipper extends over $1213 \lesssim s \lesssim 1231$ m in the raising region of the vertical orbit separation bump (the y_{co} curve, right vertical axis) at RHIC IP10. There the spin is vertically tilted (left vertical axis) by $\approx 1.8^o$ at injection (A), $\approx 2.6^o$ at store (B) [8].

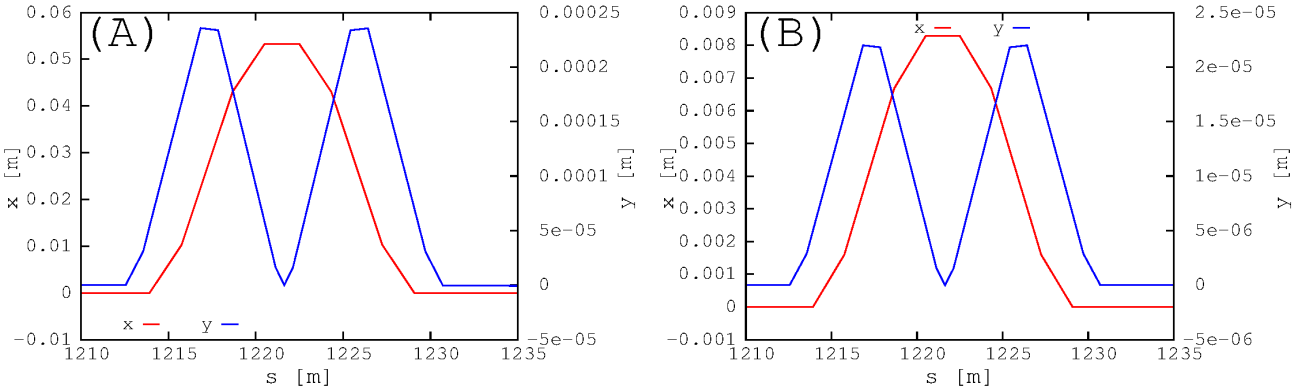

Figure 7: Geometry of the horizontal (left vertical axes) and vertical (right axes) orbit bumps over the spin flipper region $1213 \lesssim s \lesssim 1231$ m, in the maximum amplitude configuration here. (A) 23.8 GeV, (B) 255 GeV.

3.2 Optical Functions

The optical functions in the simulations are displayed in Fig. 8. A special feature of the APEX optics is in the modulation of the dispersion function, by the $\gamma_{\rm tr}$ quadrupoles as they are used to control D'_{x} at both RHIC snakes.

Note that RHIC detector magnets, STAR (solenoid) and PHENIX (a dipole oriented with field longitudinal) are absent from the simulations. Their effect on the stable spin precession axis $\vec{n}_0$ is negligible [6].

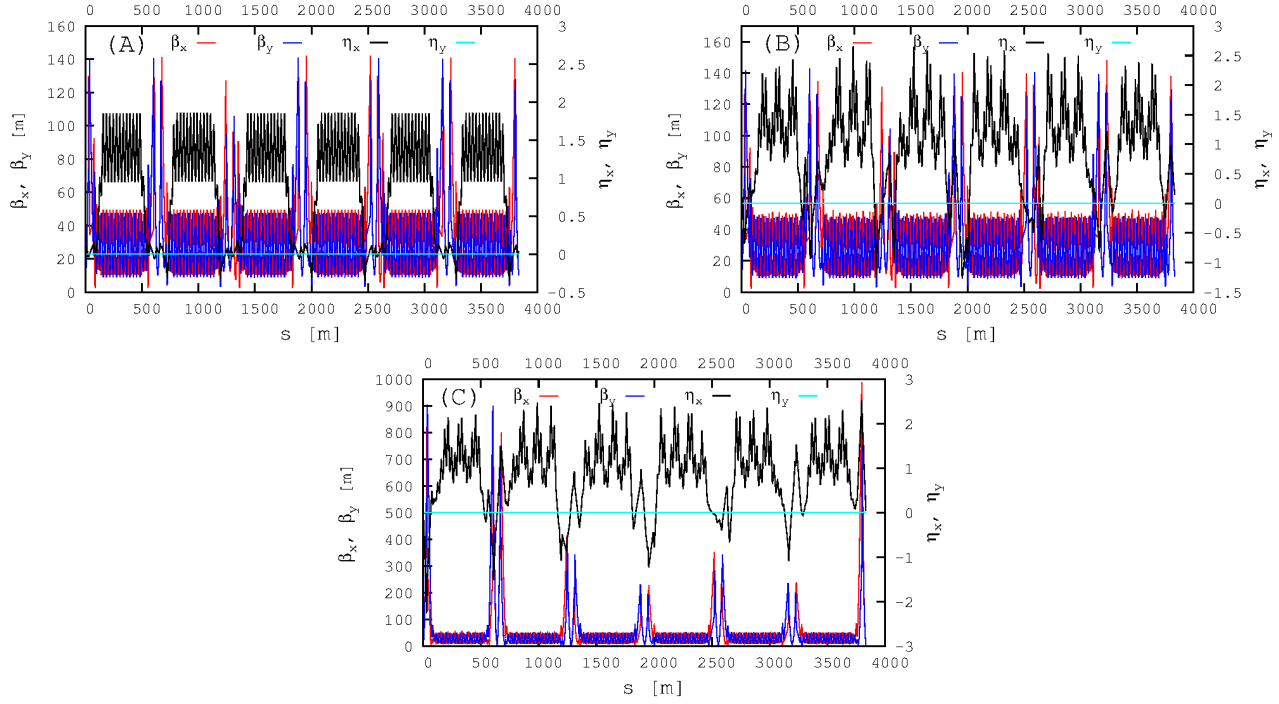

Figure 8: RHIC Blue optics. (A, B) at injection, $\nu_x = 28.695$, $\nu_y = 29.687$, $\beta^*_{\mathrm{x,y}} = 10\,\mathrm{m}$, $\xi_{\mathrm{x,y}} \approx 5$; (C) at store, $\nu_x = 28.689$, $\nu_y = 29.684$, $\beta^*_{\mathrm{x,y}} \approx 1.4\,\mathrm{m}$, $\xi_{x,y} \approx 5$. In (A), case of regular operation optics, the $\gamma_{\rm tr}$ quadrupoles are off, $D_x(s)$ is not modulated, $\mathrm{D}'_{\mathrm{x}}(\mathrm{s})$ values at snake 1 and snake 2 differ by 63 mrad. In (B) and (C), the horizontal dispersion is modulated under the effect of the $\gamma_{\rm tr}$ quadrupoles to bring $|\Delta \mathrm{D}'|$ down to respectively 13 mrad and 9 mrad.

3.3 Single particle tracking

The single particle tracking through the resonance was used to verify the Spin Flipper setup. The output tracking files (zgoubi.fai) were set to contain particle(s) coordinates at each turn at IP6. Here the stable spin direction is pretty much vertical for all the particles. Hence the initial spin direction of all the particles was chosen to be exactly vertical.

Resonance crossing

Fig. 9 shows that indeed the resonance condition happens when the spin tune is equal to the frequency of the oscillator. Additionally if the crossing speed is so low that the resonance condition is satisfied multiple times during the frequency sweep, the spin undergoes multiple flips. In these plots the dp/p simulation output was used to calculate the spin tune oscillations using Eq. 7. The average value around which the spin tune oscillates was derived from the Fourier transform of the horizontal (or longitudinal) spin component at IP6. To obtain a clear peak in the FFT spectrum, the Spin flipper and RF were turned off, plus the particle was launched with the spin in the horizontal (or longitudinal) plane and tracked for few thousand turns. An example of the FFT is shown

in Fig. 10. There are two peaks showing around 0.5. A tracking with the well balanced Spin Flipper on and the oscillator range set to cover both peaks was used to determine which peak is the SF resonance, the spin flip occurs, and which one is its mirror image.

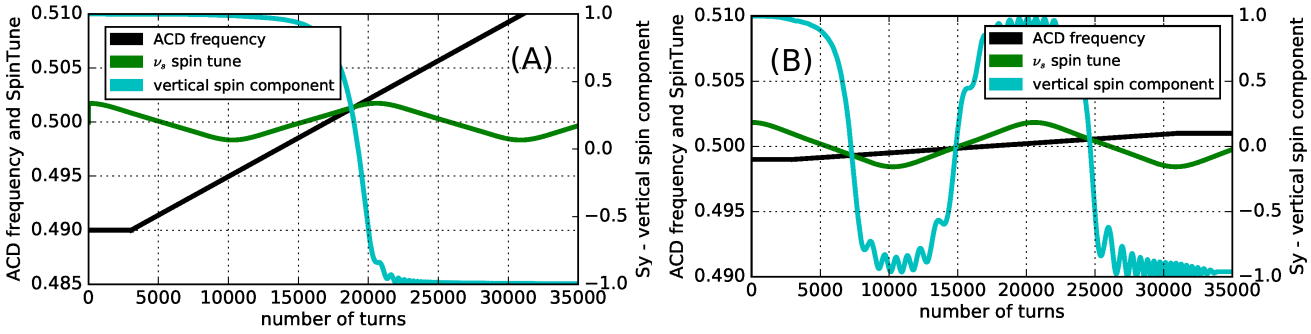

Figure 9: Crossing the resonance. The single particle simulations were used to verify the spin flipper setup, namely the resonance condition, by varying the crossing speed. The spin tune varies due to the synchrotron motion (Eq. 7). (A) Larger crossing speed. There is only one resonance condition when the $\nu_{\rm osc} = \nu_{\rm s}$. Hence the spin flips only once. (B) Lower crossing speed. There is more than one resonance condition, which causes the spin to flip multiple times.

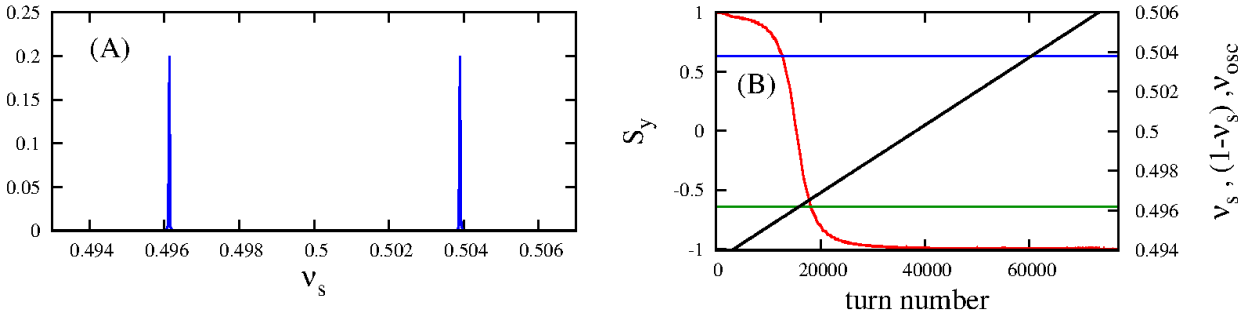

Figure 10: Spin tune calculation. (A) Fourier transform of the horizontal spin component at IP6 yields the frequency spectrum, showing two peaks around 0.5. (B) particle tracking with Spin Flipper on and the oscillator frequency covering both peaks is used to determine which of these peaks is the spin tune and which is its mirror image.

Mirror resonance

During the FY17 APEX studies the Static Spin Tune Scan showed no resonance excited where the mirror resonance would be for 23.8 GeV, but the 255 GeV data suggests otherwise [4, Fig. 2].

The simulations of the well balanced spin flipper show that the mirror resonance cancels out as can be seen in Fig. 10B, since the spin of the particle is not affected when the frequency of the oscillator is swept through the mirror resonance $\nu_{\rm osc} = (1 - \nu_{\rm s})$. It was verified by simulations that the mirror resonance gets excited, as shown in Fig. 11, in the following cases of the Spin Flipper being un-balanced:

- not-closed ACD vertical bump, particularly when the strength of the second dipole of first ACD bump was changed.
- a difference in the frequency range of the two ACD bumps. Two ACD bumps had a slightly different frequency range.

- mis-setting of the ACD1-3−ACD3-5 relative phase as given by Eq. 3.

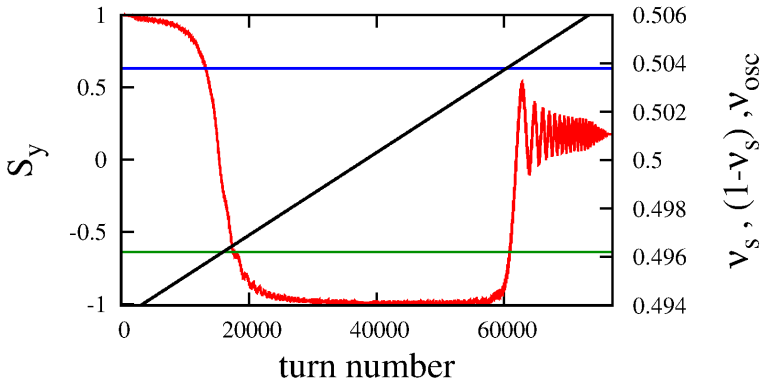

Figure 11: The tracking was setup for the oscillator frequency range to cover both the ν_s and $(1-\nu_s)$. The spin flipper error was introduced in the simulation setup, mis-setting of the ACD1-3−ACD3-5 relative phase in this case. This excites the mirror resonance.

Spin Tune dependence

The validity of Eq. 7 was further tested by doing a $\Delta p/p$ and $\Delta D'$ scan. Single particles with different momenta were tracked through a lattice with high $\Delta D' = 30$ mrad during the $\Delta p/p$ scan. The FY17 lattice with different $\Delta D'$ was used to track single off-momentum (high $\Delta p/p = 0.0005$) particles for the $\Delta D'$ scan. The spin tune was determined from the FFT of the horizontal spin component, using tracking files in which the Spin flipper and RF are off. Fig. 12 shows a good agreement between the simulations at 255 GeV and the values obtained using Eq. 7.

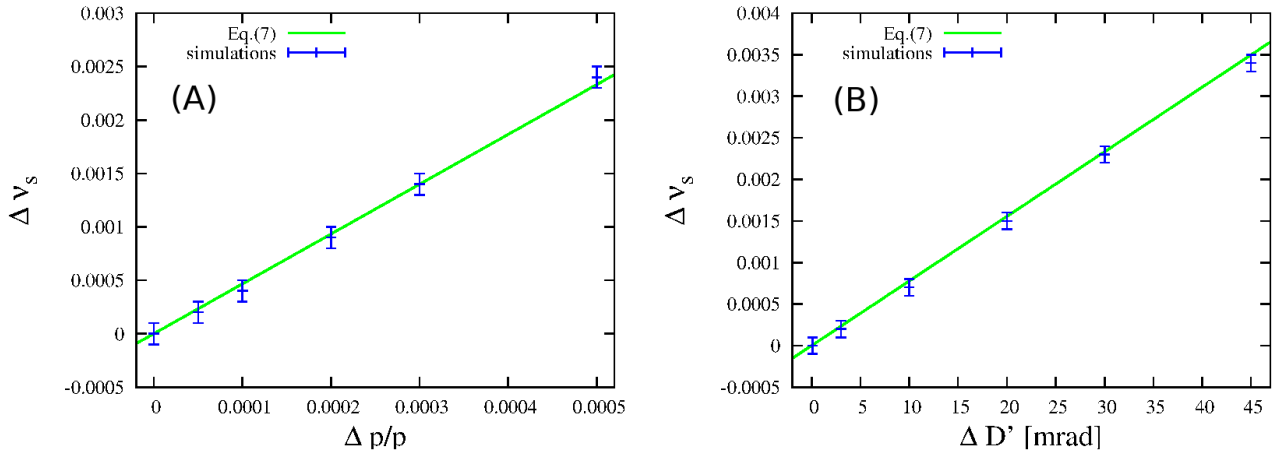

Figure 12: The Spin Tune dependence on $\Delta p/p$ and $\Delta D'$ is linear and agrees well with the Eq. 7. These simulations were done at 255 GeV. with the Spin Flipper and RF off. The spin tune was derived from the FFT of the horizontal spin component, the spin tune error corresponds to one FFT bin. (A): $\Delta p/p$ scan. Single particles with different momenta were tracked through a lattice with high $\Delta D' = 30$ mrad in order to obtain the observable spin tune changes for different momenta. (B): $\Delta D'$ scan. The FY17 lattice with different $\Delta D'$ was used to track single off-momentum (high $\Delta p/p = 0.0005$) particles.

4 Multiparticle tracking

The multiparticle tracking was done using the NERSC computational facility [7].
Typically 960 particles per ”bunch” were tracked. The particle initial distribution was setup to match the APEX transverse and longitudinal emittances, which are shown in Tab. 1. The initial spin of all the particles was set to be purely vertical. Three plots of Fig. 13 show an example of the transverse and longitudinal phase space during tracking of 40 particles undergoing spin flip at the injection energy. It is worth mentioning that the emittance is conserved during the spin flip and as can be seen the longitudinal phase distribution matches the WCM measurements Fig. 4. The forth plot shows a development of the vertical spin component; the red traces correspond to tracking of 40 random particles, while the blue trace is an 960 particle average.

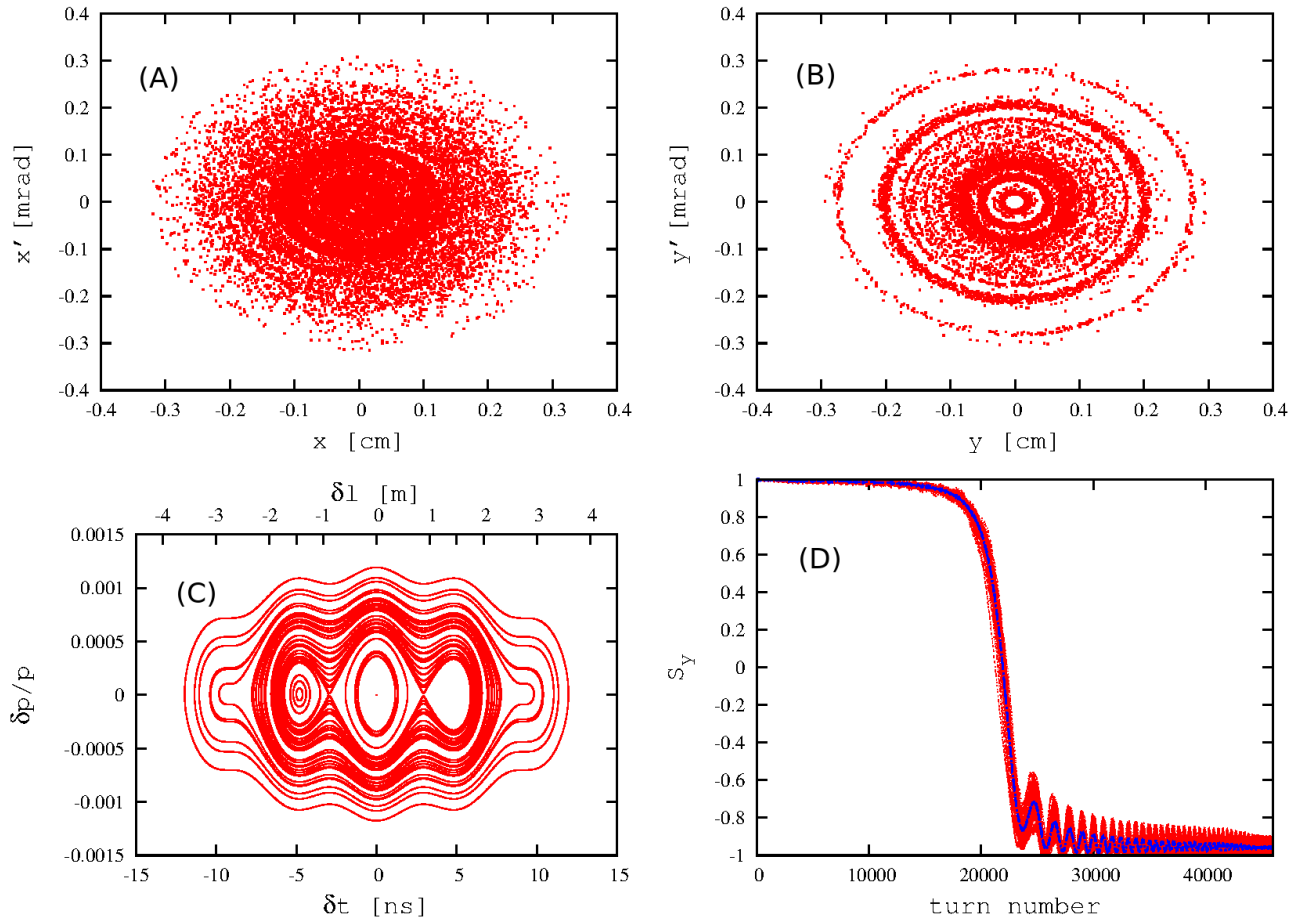

Figure 13: An example of the multiparticle tracking at 23.8 GeV with β^*= 10 m ΔD′ = 3.45 mrad and 0.5 s sweep duration. Red traces show tracking of 40 random particles, blue is the 960 particle average. (A)-(C) horizontal, vertical and longitudinal phase space. (D) Vertical spin component versus number of turns.

4.1 Initial and final polarization

To calculate the spin flip efficiency it is important to determine the initial polarization, P_i. Fig. 14 shows oscillations of the average vertical spin component during the first fifty turns, when the AC dipole is still off. The initial polarization was set as the value around which the average vertical spin component oscillates, its values are summarized in Tab. 3 for different energies. The slight depolarization occurs at 255 GeV, which is likely caused by the neighboring resonances.

The final polarization, P_f, was set as a value around which the average vertical spin coordinate at the end of tracking when the AC dipole is already ramped down.

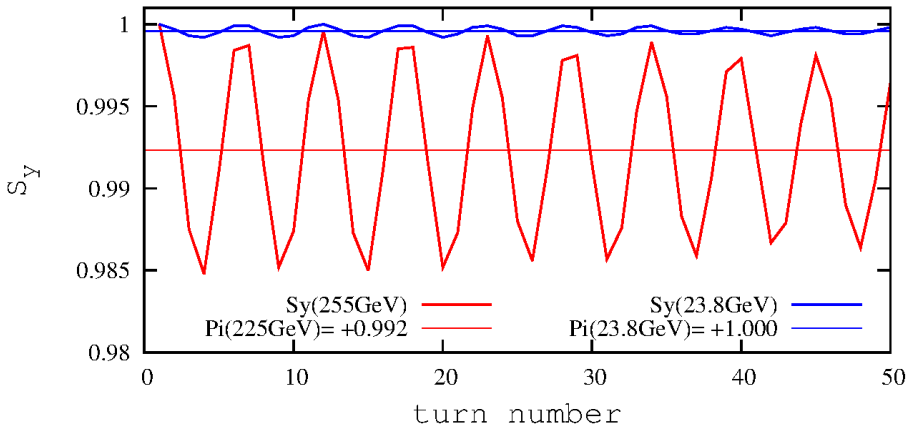

Figure 14: The initial polarization for 23.8 GeV and 255 GeV.

Table 3: The initial polarization

energy	23.8GeV	255GeV
P_i	+100%	+99.2%

4.2 AC dipole up/down ramp

During the APEX the AC dipole up/down ramp was 1.5 s long as mentioned in Section 2. In order to shorten the simulation time, the effects of the ACD ramp duration onto the spin flip efficiency were studied. The spin flip simulations with the 0.2 s sweep time and $|\Delta D'| < 1\text{nrad}$ at 255 GeV were used for this purpose. The AC dipole up/down ramp was varied between 1 and 117,000 turns. The results are shown in Fig. 15. One can see that there are almost no oscillations of the average vertical spin component for the 3,000 turn ramps, thus most of the simulations were done for the ramps lasting 3,000 turns instead of 117,000 turns with marginal effect on the final polarization. As an example, Fig. 16 shows the evolution of the vertical spin coordinate for the 3000 and 117,000 turn AC dipole ramps.

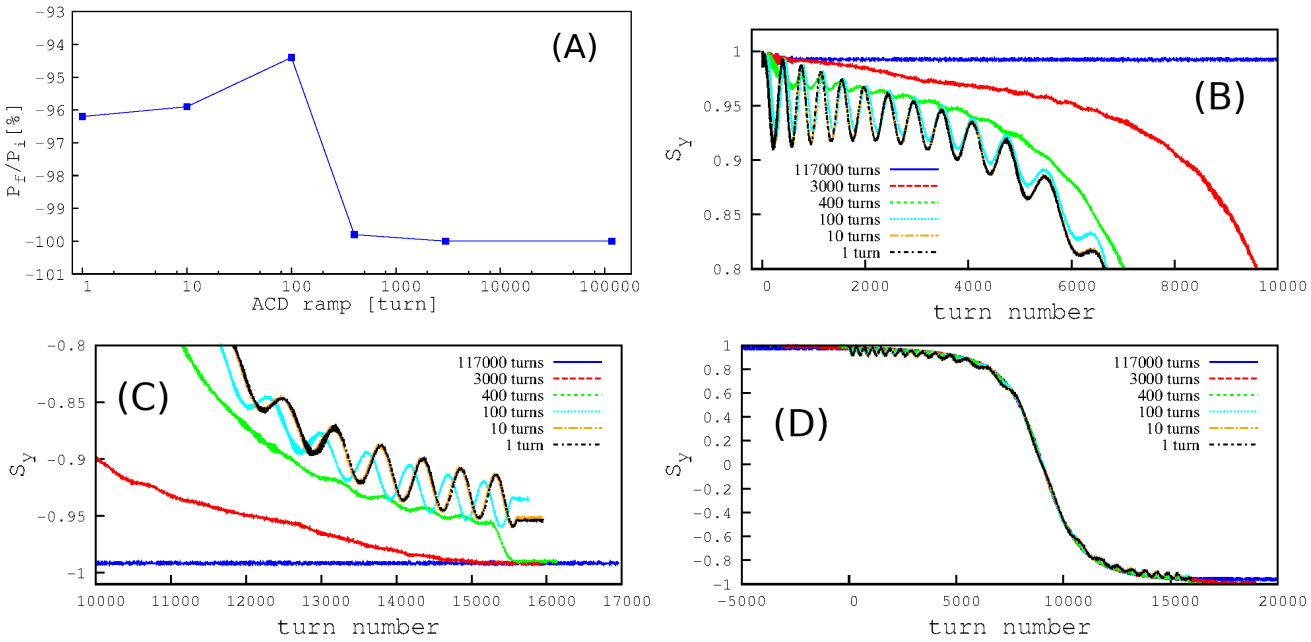

Figure 15: Varying the ACD up/down ramp duration: (A) Spin flip efficiency as a function of ACD up/down ramp length; (B) Up-ramp: flips aligned such that turn=0 is the start of the ACD up-ramp; (C) Down-ramp: flips aligned such that turn=15600 is the END of the ACD ramp down (which is pretty much P_f - final polarization); (D) Frequency sweep: flips aligned such that turn=0 is the start of the frequency sweep.

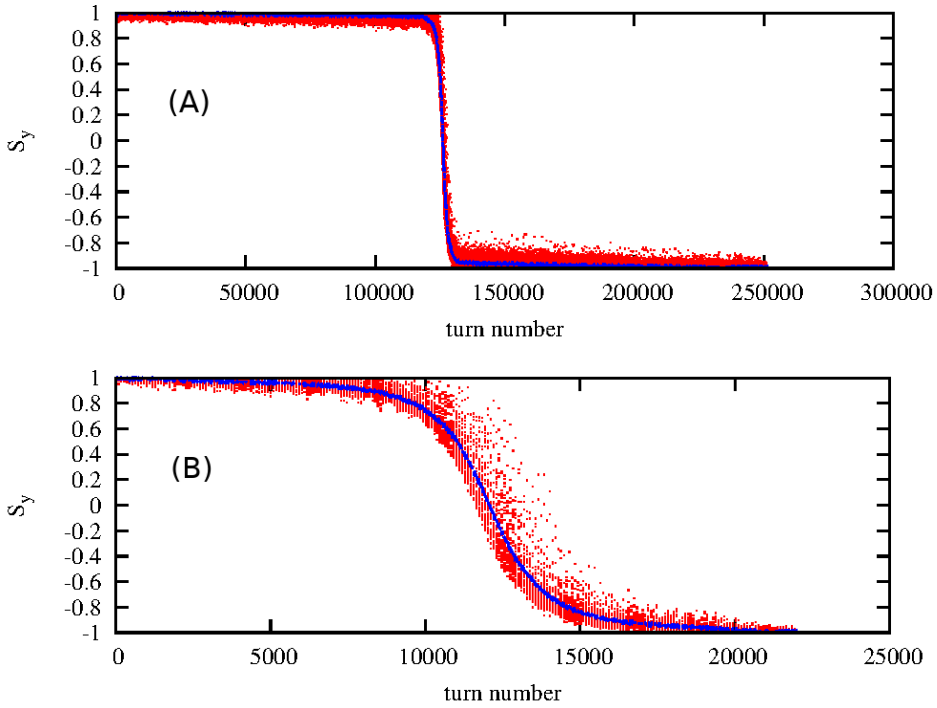

Figure 16: Examples of the spin flip simulations: (A) 1.5 s AC dipole up/down ramp (117,000 turns); (B) 3000 turn ramp. Most of the simulations were done for the ramps lasting 3,000 turns instead of 117,000 turns with marginal effect on the final polarization.

5 Comparison of the FY17 APEX Experimental Data with Simulations at Injection Energy

This note compares only simulations with measurements during which the oscillator frequency was swept. There were additional experiments done such as Static Spin Tune scan [4].

5.1 Sweep Time Scan at Injection energy

There were three spin flip efficiency measurements performed for $\Delta D' = 3.45$ mrad and $\Delta\nu_{osc} = 0.005$ at the 23.8 GeV, with the sweep time being varied (0.5s, 1.0s and 3.0s). The simulations, set up for these conditions, agree with the measurements within the errors of the APEX measurement, as shown in Tab. 4 and Fig. 17. The simulations, with $|\Delta D'| < 1$nrad[1], were done to see how close to 100% spin flip efficiency one can get. These simulations as well as the measured data show deviations from Froissart-Stora formula. These deviations are greater for longer sweep time and are $\Delta D'$ dependent. The additional simulations were performed with $|\Delta D'| <$ 1nrad, 3 s long sweep time and RF off, the spin flip efficiency of such setup matches with the Froissart-Stora predictions. This result suggests that the longitudinal motion plays additional role during the spin flip even in the case when $|\Delta D'|$ is small enough that multiple resonance crossings do not occur.

Table 4: Sweep Time Scan at Injection energy, $\Delta D' = 3.45$ mrad and $\Delta\nu_{osc} = 0.005$.

Sweep Time	**0.5 s**	**1.0 s**	**3.0 s**
P_f/P_i(APEX) [%]	-95.0±2.6	-97.5±1.9	-92.0±1.5
P_f/P_i(simulations) [%]	-95.8	-97.9	-94.4

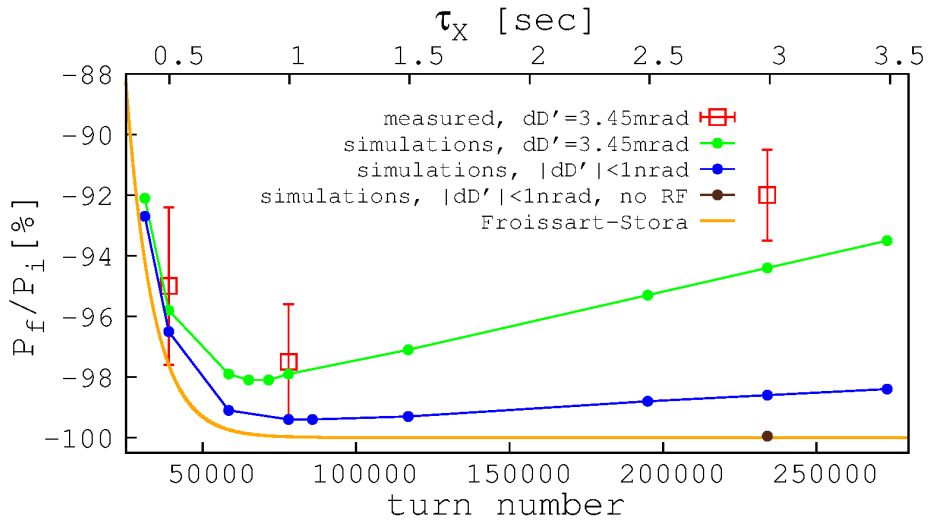

Figure 17: Dependence of spin flip efficiency on sweep time duration, for different $\Delta D'$ values, including measured (red, empty squares) and simulated (solid markers) data, at 23.8 GeV, shows a good agreement between measurements and simulations. The optimal sweep time appears to be around 1 s with $P_f/P_i = -99.4\%$ for $|\Delta D'| <$ 1nrad in simulated data.

[1]This value was derived from the Zgoubi standard output file, where D'_x values are printed and show $nrad$ as their last decimal point.

5.2 ΔD$'$ Scan at Injection energy

A difference of the dispersion function derivatives at the two snakes, ΔD$'$, affects the spin tune spread of the particle bunch, as given by Eq. (7). During APEX, with the sweep time set to 3 seconds, ΔD$'$ was varied from nominal 60 mrad down to 3.45 mrad to study its effects on the spin flip efficiency. Tab. 5 and Fig. 18 show a good agreement between experimental data and simulations. The low spin flip efficiency for high ΔD$'$ is caused by multiple resonance crossings as illustrated in Fig. 19. The additional simulations, with 1 second sweep time, show that the optimal sweep time can be used to improve the spin flip efficiency, yielding $P_f/P_i = -99.4\%$ for $|\Delta\text{D}'| < 1\text{nrad}$. One can see that the 1s and 3s simulations plotted lines cross at around 40 mrad in Fig. 18. This surprising result is in more details explored in Fig. 20. This plot shows the average vertical spin component versus the number of turns. It appears that some interference exists in the 1 second case.

Table 5: ΔD$'$ Scan at Injection energy, with $\Delta\nu_{\text{osc}} = 0.005$. and $\tau_{\text{X}} = 3\,\text{s}$

ΔD$'$[mrad]	**3.45**	**10**	**44**
$\text{P}_\text{f}/\text{P}_\text{i}$(APEX) [%]	-92.0±1.5	-68.1±2.7	-8.5±2.8
$\text{P}_\text{f}/\text{P}_\text{i}$(simulations) [%]	-94.4	-62.9	-12.0

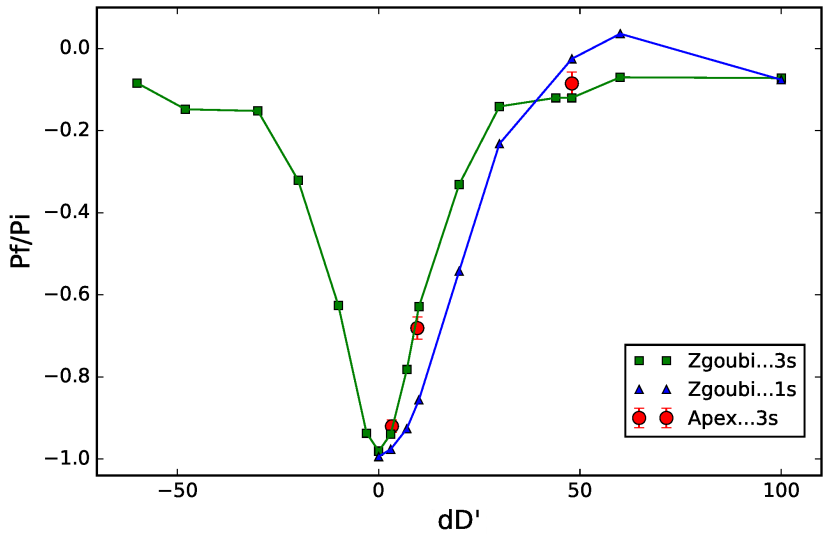

Figure 18: ΔD$'$ scan at 23.8 GeV with $\Delta\nu_{\text{osc}} = 0.005$. The measured data and simulations ($\tau_{\text{X}} = 3\,\text{s}$) show a good agreement. The simulation for the optimal sweep time ($\tau_{\text{X}} = 1\,\text{s}$) yield $P_f/P_i = -99.4\%$ for $|\Delta\text{D}'| < 1\text{nrad}$. Increasing $\Delta\nu_{\text{osc}}$ improves the spin flip efficiency by less than $0.1\ \%$.

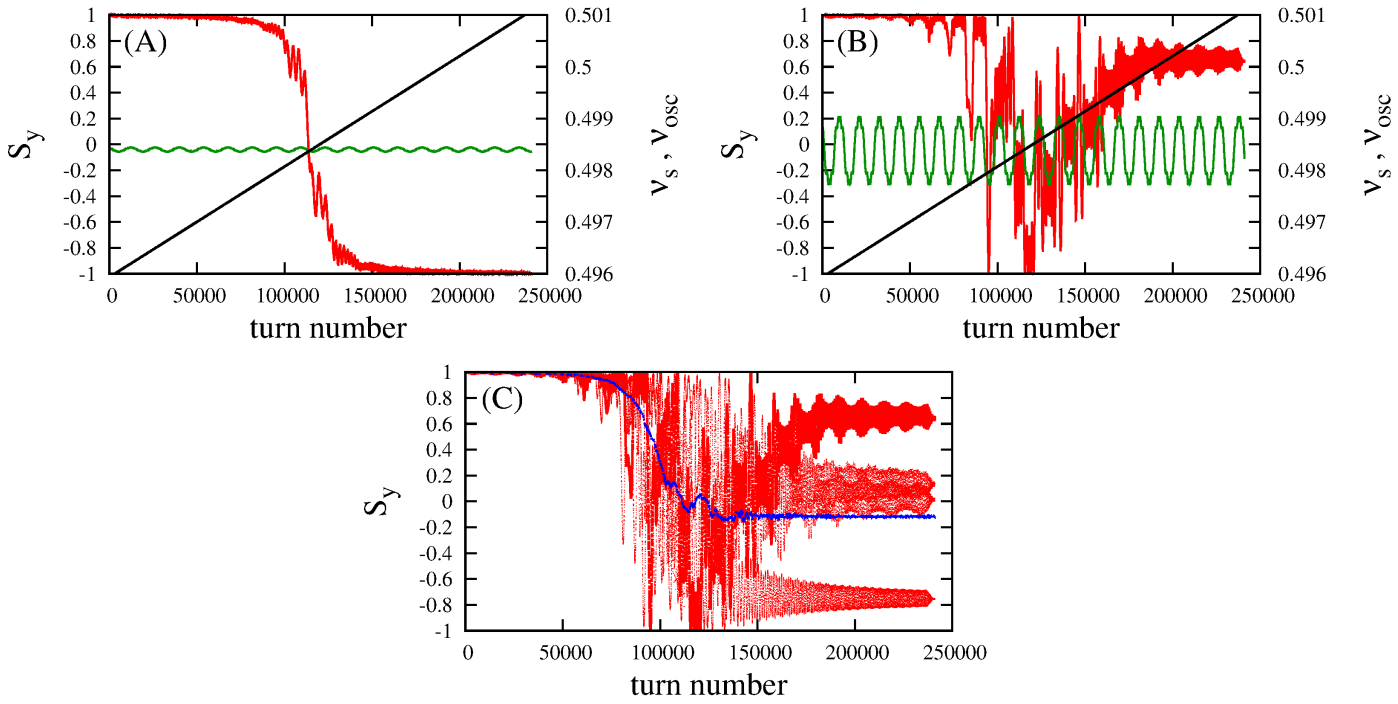

Figure 19: Particle tracking for different values of $\Delta D'$. (A) A single particle tracking for $\Delta D' = 3.45$ mrad. The resonance is crossed only once. (B) A single particle tracking (same initial coordinated as in (A)) for large $\Delta D' = 44$ mrad causes a large spin tune oscillation $\delta\nu_s$ (Eq. 7) resulting in multiple resonance crossings. (C) Multiple particle tracking for large $\Delta D' = 44$ mrad. Sample spin motion (red) and average vertical spin component of a 10^3 particle bunch (blue). The polarization is lost during the spin flip in this case.

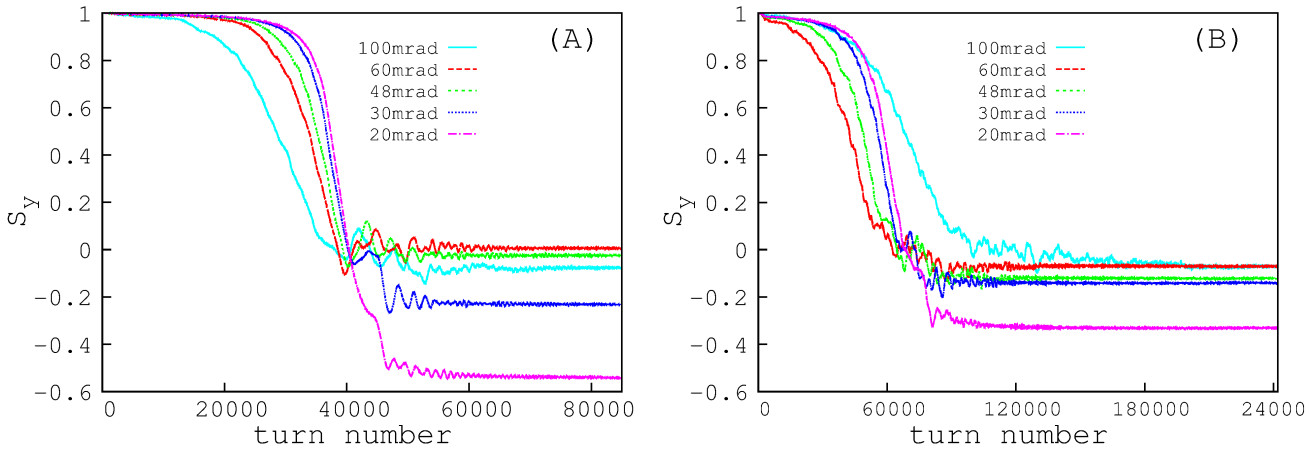

Figure 20: The average vertical spin component versus number of turns at 23.8 GeV, with $\Delta\nu_{osc}$=0.005, simulations results for $\Delta D'$ ranging from 20 to 100 mrad. (A) 1 second sweep time shows signs of some interference (B) 3 second sweep time.

6 Comparison of the FY17 APEX Experimental Data with Simulations at Store Energy

The FY17 APEX store measurements were done at 255 GeV at the end of the energy ramp, before re-bucketing, thus using 9MHz+197MHz RF system. The Zgoubi simulations were set up to match the APEX conditions, except for a small energy difference. The APEX was performed at $G\gamma = 487.0$ while most of the simulations were done at $G\gamma = 487.5$. The additional simulations show that such a small energy difference does not affect the SF efficiency, only the initial polarization and the "spin flip width" slightly change. See App.A for details.

6.1 Sweep Time Scan

The Sweep time scan at 255 GeV was measured for $\Delta D' = 0.12$ mrad, $\Delta\nu_{osc} = 0.005$ and $\tau_X = 0.5$ and 1.0 s during the APEX. The simulations using FY17 lattice were performed for these conditions, the 0.5 s measurement agrees with the simulations within 1 sigma, but the result for 1 s simulations shows a disagreement with measurement greater than 1 sigma, as shown in Tab. 6 and Fig. 21. Nevertheless one can estimate the optimum sweep time to be around 0.2 s for $\Delta\nu_{osc} = 0.005$ with $P_f/P_i(FS) = -100.0\%$ according to simulations. Making the ACD ramp or $\Delta\nu_{osc}$ longer changes the spin flip efficiency by less than 0.1%. The additional simulations, with $|\Delta D'| < 1$nrad, show the deviations from Froissart-Stora formula for longer sweep time (for 3 s sweep time: $P_f/P_i(sim) = -99.2\%$ and $P_f/P_i(FS) = -100.0\%$), but if the RF is turned off, the simulations results agree with the Froissart-Stora predictions. Similar to the simulations at injection, there is additional effect on spin flip efficiency from momentum spread or spin tune spread beside Eq. 7.
The following subsection describes the attempts to match the simulation results with the measured data.

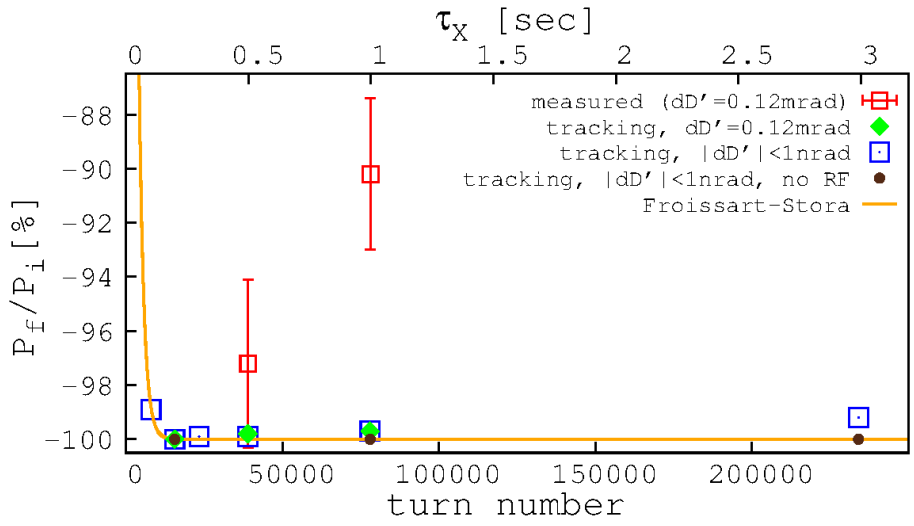

Figure 21: Dependence of spin flip efficiency on sweep time duration, for different $\Delta D'$ values, including measured (red, empty squares) and simulated data using FY17 lattice, at 255 GeV. The optimal sweep time seems to be 0.2 s yielding $P_f/P_i(FS) = -100.0\%$ for shown simulations with RF on. The simulations with $|\Delta D'| < 1$nrad and 3 s sweep time disagree with Froissart-Stora predictions, even though no multiple resonance crossings should be happening according to Eq.7; the RF voltage needs to be turned off in order to reach an agreement.

Table 6: The Sweep Time Scan at 255 GeV. A comparison of the Experimental Data and Simulations for $\Delta D' = 0.12$ mrad and $\Delta\nu_{osc} = 0.005$ is shown here.

Sweep Time [s]	**0.5**	**1.0**
P_f/P_i(APEX) [%]	-97.2 $\pm$ 3.1	-90.2 $\pm$ 2.8
P_f/P_i(simulations) [%]	-99.8	-99.7

6.1.1 Modifying the simulation setup in order to explain Time Scan data at 255 GeV

Attempts were made to match the simulation results with the measured data by changing various parameters such as $\Delta D'$ and $\Delta p/p$ or/and by introducing errors to RHIC lattice or/and Spin Flipper.
Tab. 7 summarizes the results of these attempts. The simulations with $\Delta D' = 20$ mrad are very close to the measured data but are not a likely explanation, since the error on $\Delta D'$ measurement is 0.1 mrad. The most likely scenario explaining the measured data seems to be that the Spin Flipper was not balanced, affecting the SF efficiency mainly for the 1.0 s case.

The fact of polarization drop at mirror resonance location at store, and not at injection, in the static spin tune scan [4] suggests that there might be imperfection in the AC dipole orbit closure, as discussed in Section 3. The orbit at the Spin Flipper is not same at two energies due to the -25 mm horizontal injection bump, and the different amplitudes of the DC and AC bumps 7.

In simulations the ACD bump error was introduced by changing the maximum amplitude of the 2^{nd} AC dipole from the full strength of $B_{osc}L$ = 0.0101 T.m down to 0.0050 T.m. The behavior of the average vertical spin component during the spin flip with the AC dipole error introduced is shown in Fig. 22. The SF efficiency of the 1.0s APEX measurement agrees with simulations when a 30% error to the 2^{nd} AC dipole is introduced.

6.2 Partial resonance sweep

Incomplete flip occurs if the $\Delta\nu_{osc}$ swing only partially covers the AC dipole induced resonance. Some of the APEX measurements happen to fall into this configuration. They are considered, too, as an opportunity for additional simulation benchmarking.

Spin tune The APEX included measurements with the Siberian snake currents set at 321 A and 95 A which theoretically should correspond to ν_s=0.4968 [8]. The nominal snake currents are 323 A and 100 A (this theoretically yields ν_s=0.4982). The difference in the snake settings should result in a spin tune shift of $\delta\nu_s$=-0.0014.

The spin tune at 255 GeV was measured for the nominal snake settings (323 A and 100 A) to be $\nu_s = 0.496125 \pm 0.000257$. The spin tune for snake currents of 321 A and 95 A was not measured, but it should be around ν_s=0.4947, if we consider how the spin tune shifts depending on the snake settings.

Spin Flip Two spin flip measurements were performed successively at 255 GeV, with $\Delta D'$=3 mrad, sweep time τ_X=3 s and $\Delta\nu_{osc}$=0.005. During the first spin flip, the AC dipole frequency range was set to 0.495-0.500, which is not covering the whole resonance (given ν_s=0.4947). The spin flip efficiency was measured $P_f/P_i = (-32 \pm 4)\%$.

The AC dipole frequency range was changed to 0.493-0.498 yielding the spin flip efficiency $P_f/P_i = -(78 \pm 20)\%$ for the second spin flip.

Simulations Sets of simulations with various distances between driving tune and spin tune have been performed (Fig. 23) regarding the first and the second spin flip, showing a good agreement with the measured values. Distance to Spin Tune is defined as the lower limit of the driving tune range minus the spin tune. A negative value means the spin tune is inside the driving tune sweep range. Difference between the simulations at $G\gamma$ 487.0 and 487.5

Table 7: An attempt to explain the Sweep Time scan data at 255 GeV by changing the simulations setup. The table shows $\mathrm{P_f/P_i[\%]}$ for various conditions.

Sweep Time	**0.5 s**	**1.0 s**
APEX results	-97.2 $\pm$ 3.1	-90.2 $\pm$ 2.8
Nominal simulations	-99.8	-99.7
Changing $\Delta\mathrm{D}'$ to 20 mrad	-95.9	-90.2
Changing $\Delta\mathrm{p/p}$ to 0.6e-3, while at the same time adjusting the voltage on the RF cavities in order to preserve longitudinal phase distribution	-96.9	-93.4
Changing spin tune by 0.001 (making the spin flip less centered)	-	-99.6
Making the vertical emittance twice bigger. Note: this causes $\mathrm{P_i}$ drops from 0.992 to 0.985.	-	-99.6
Introducing the 5 mm vertical separation bump at IP10. The spin flipper is on the rising edge of this bump. This should not and does not affect SF efficiency.	-99.8	-
Introducing an 15%-ACD bump error, by reducing the strength of the 2^{nd} AC dipole by 15%.	-	-98.9
IP10 bump (same as above) plus 15%-ACD bump error (same as above).	-99.3	-98.7
RHIC Y-orbit error in vertical trim supplies which causes the closed orbit to have 1mm vertical oscillations in arcs. Note: this causes $\mathrm{P_i}$ drops from 0.992 to 0.989.	-	-99.4
RHIC Y-orbit error (same as above) plus 15%-ACD bump error (same as above)	-99.1	-98.2
IP10 bump (same as above) plus RHIC Y-orbit error (same as above) plus 15%-ACD bump error (same as above).	-	-98.2
IP10 bump (same as above) plus 30%-ACD bump error (introduced by reducing the strength of the 2^{nd} AC dipole by 30%).	-71.7	-90.8
IP10 bump (same as above) plus RHIC Y-orbit error (same as above) plus 30%-ACD bump error (same as above).	-	-89.2
IP10 bump (same as above) plus 50%-ACD bump error (introduced by reducing the strength of the 2^{nd} AC dipole by 50%).	-98.1	-96.7

is contributed to the "Spin Flip width" which is discussed in more details in Appendix A. Fig. 24 demonstrates how the polarization is affected during the partial sweep. The distance to spin tune is 0.0001 in this case, which means that the spin tune is just outside of the oscillator range. Usually one would expect that the spin flip can only happen when the spin tune is covered by the driving tune sweep range. In reality, due to the spin tune spread, the partial spin tune flip can still happen if the spin tune of some portion of the beam is in the driving tune sweep range.

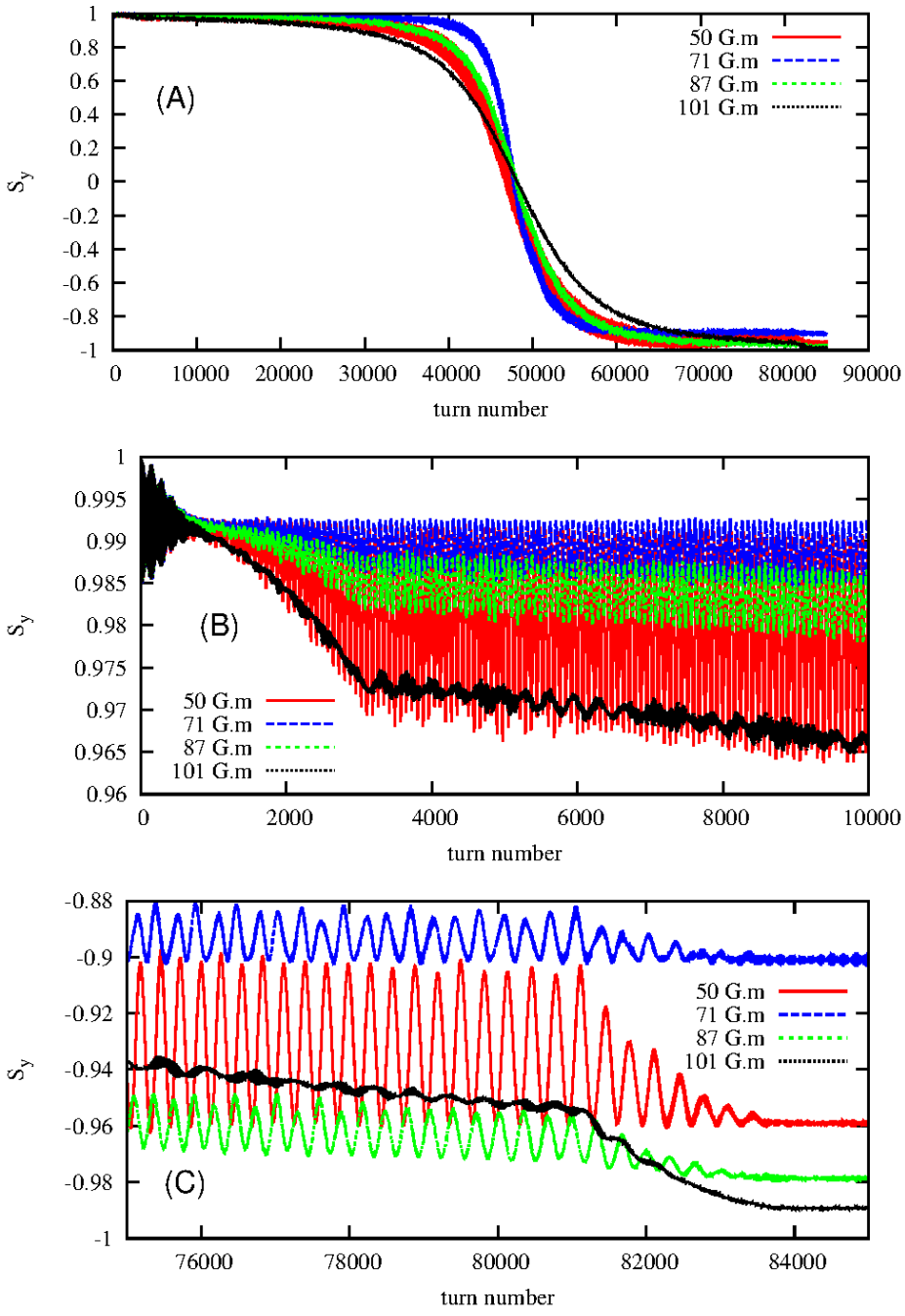

Figure 22: The average vertical spin component oscillates throughout the spin flip and the SF efficiency can be negatively affected when the ACD bump is not closed. The maximum strength of the 2$^{\text{nd}}$ AC dipole was varied from 0.0101 T.m (no error) down to 0.0050 T.m (50% error). (A) Spin Flip with 1 second sweep time at 255 GeV. (B),(C) - zoom on the beginning and the end of tracking.

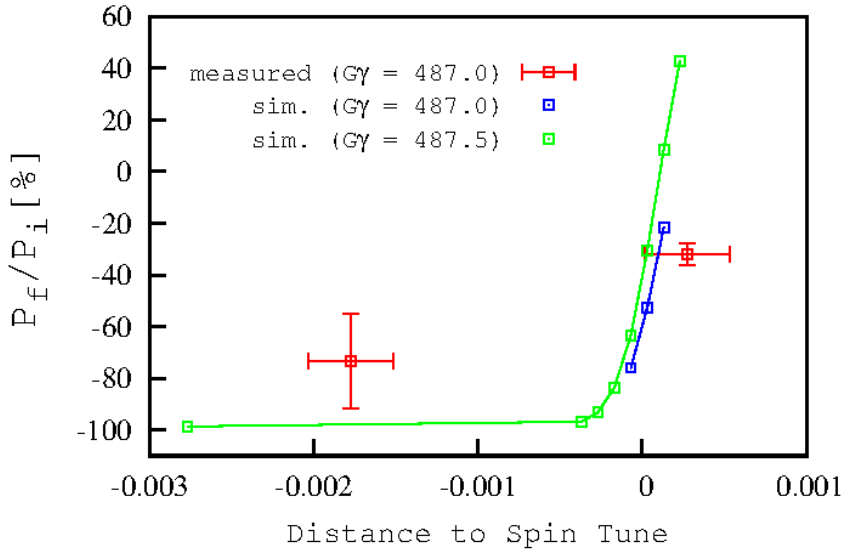

Figure 23: Partial resonance sweep. The spin flip efficiency depends on how far the spin tune is outside of the oscillator range. The driving tune sweep range is 0.005, $\Delta D' = 3\mathrm{mrad}$, $\tau_X = 3\,\mathrm{s}$ at 255 GeV. Red - measured data; Black - simulations. The simulations were done for $G\gamma$ equal to 487.0 and 487.5; the APEX measurements were done at 487.0.

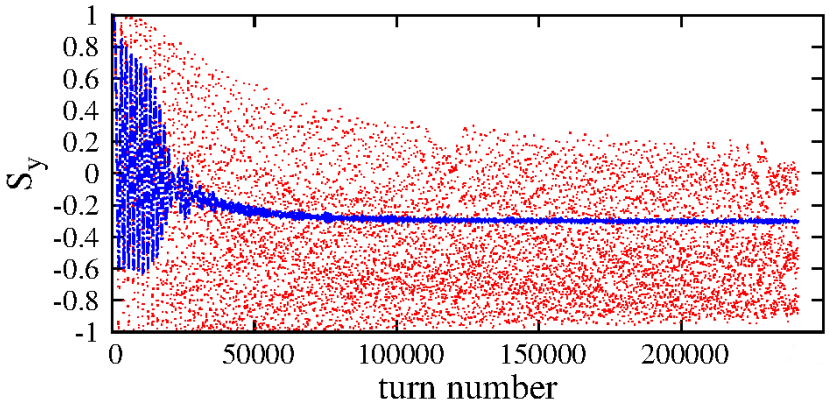

Figure 24: Simulation of the spin flip when the whole resonance is not covered, causing an asymptotic polarization of $P_f = -0.3$, from an initial $P_i \approx +1$. Red - vertical spin component of individual particles; Blue - average vertical spin component of the 10^3 particles.

7 Simulations at 255 GeV after rebucketing (28MHz+197MHz)

The APEX 255 GeV measurements were done before rebucketing, using 9MHz and 197MHz RF systems. During the physics stores the nominal RF setup uses two 28MHz cavities per ring at 140kV each, plus one 197 MHz cavity per ring at 150 kV each.

The following simulations were setup for 28MHz+197MHz RF conditions, using the FY17 lattice at $G\gamma = 487.5$ with $|\Delta D'| < 1\mathrm{nrad}$ and $\Delta\nu_{osc}$=0.005. The longitudinal phase was set to match the WCM measurements, see Fig. 25. The new $\Delta p/p$ is equal to $\pm$0.6e-3 based on the particle tracking, given the new longitudinal phase and RF settings. The simulations show that the synchrotron period is approximately 10x smaller (0.02 s) after rebucketing compared to 0.2s before rebucketing.

Fig. 26 shows how the different RF settings affect the spin flip efficiency. The results suggest that the best spin flip efficiency would be for the sweep time <0.01 s while using the 28MHz+197MHz RF system with $|\Delta D'| < 1\mathrm{nrad}$, $\Delta\nu_{osc}$=0.005 and the Spin Flipper, of the APEX strength. But the sweep time <0.01 s is not possible to obtain with the current Spin Flipper hardware. As increasing the driving tune sweep range is another way to increase the resonance crossing speed, more simulations were done for wider $\Delta\nu_{osc}$ (see subsection 7.1).

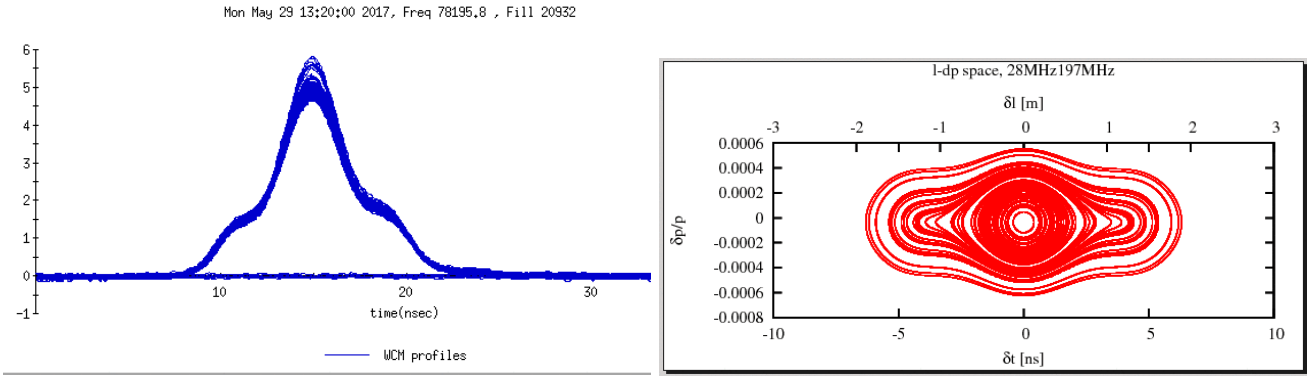

Figure 25: The simulations, at 255 GeV using the 28MHz+197MHz RF system, were setup to match the longitudinal phase with the WCM measurement. The WCM snap from one of the FY17 physics stores was used, since the APEX studies were done before re-bucketing.

7.1 The $\Delta\nu_{\mathrm{osc}}$ scan

More simulations were done to find the optimal values of the crossing time and the driving frequency range for the physics store conditions (at 255 GeV after rebucketing, with $|\Delta D'| < 1\mathrm{nrad}$). The APEX Spin Flipper strength was used for these simulations, only $\Delta\nu_{\mathrm{osc}}$ and τ_{X} were varied. Results are shown in Fig. 27. The best spin flip efficiency around 86% was reached for all simulated values of $\Delta\nu_{\mathrm{osc}}$ (0.005, 0.01, 0.02). A wide plateau where the spin flip efficiency is almost constant was observed for $\Delta\nu_{\mathrm{osc}} = 0.02$ with the crossing time being around 0.3 s, which are achievable values for the current Spin Flipper.

7.2 The stronger Spin Flipper

Simulations of the stronger Spin Flipper were done to study its effects on the SF efficiency after re-bucketing. In the following simulations the strength of the Spin Flipper was changed by increasing the magnetic field of the AC dipole up to 4 times. The maximum amplitude of the AC dipole vertical bump changed from approximately $2.2 * 10^{-5}\mathrm{m}$ to $8.8 * 10^{-5}\mathrm{m}$, as can be seen in Fig. 28.

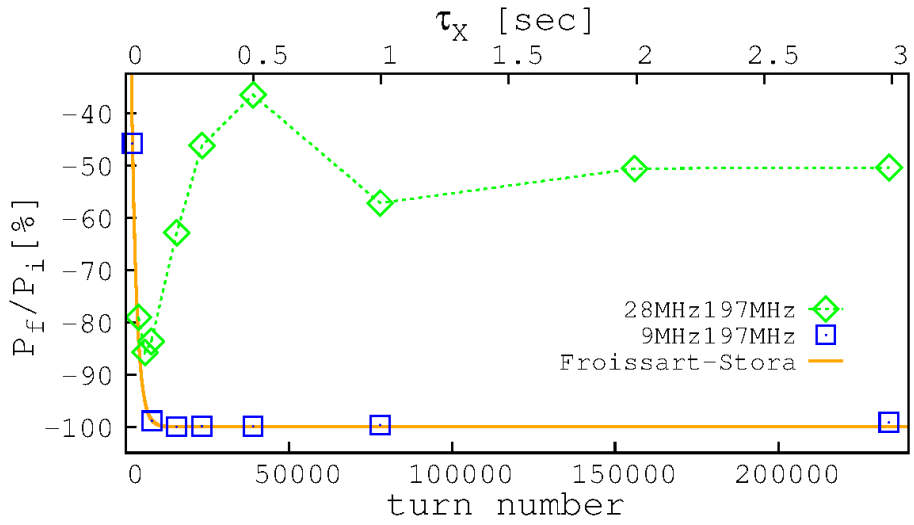

Figure 26: Effects of different RF systems, namely 9MHz+197MHz versus 28MHz+197MHz, on the spin flip efficiency. The simulations at 255 GeV, using FY14 lattice, were done for $\Delta\nu_{\rm osc} = 0.005$ and $|\Delta {\rm D}'| < 1{\rm nrad}$. The best spin flip efficiency is only around 86% for 28MHz+197MHz system for $\tau_{\rm X}$ <0.1 s.

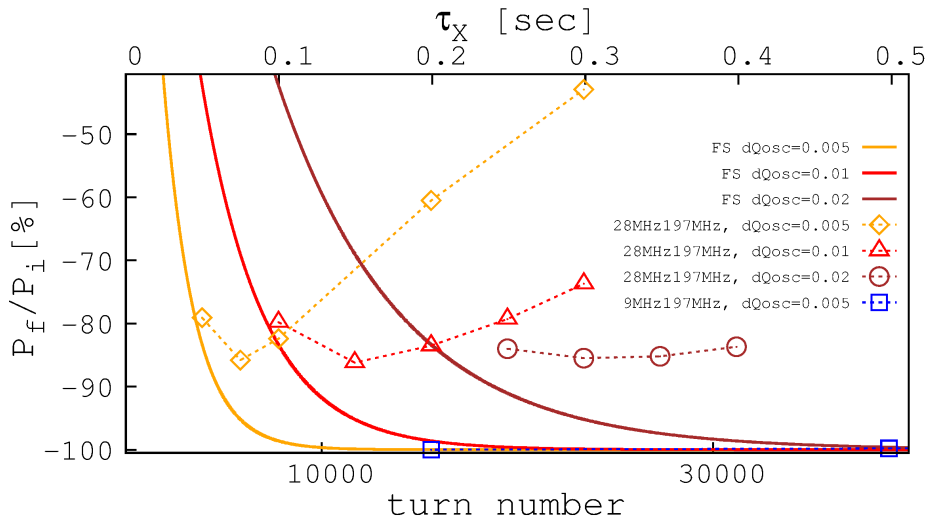

Figure 27: $\Delta\nu_{\rm osc}$ scan at 255 GeV after rebucketing was done for three values of $\Delta\nu_{\rm osc}$ (0.005, 0.01, 0.02). The best value for the oscillator frequency range is $\Delta\nu_{\rm osc} = 0.02$ with the crossing time being around 0.3 s yielding 86% spin flip efficiency according to these simulations.

The results of the simulations for $\Delta\nu_{\rm osc} = 0.02$ are summarized in Tab. 8 and Fig. 29. Tab. 9 and Fig. 30 shows results for $\Delta\nu_{\rm osc} = 0.005$. These simulations were done using FY17 lattice with $|\Delta {\rm D}'| < 1{\rm nrad}$. The spin tune $\nu_{\rm s} = 0.4962$ was set to be equal to the APEX value. The drive tune frequencies $\nu_{\rm osc} = [0.48, 0.50]$ were adjusted not to go past 0.5 for the $\Delta\nu_{\rm osc} = 0.02$ case. The drive tune frequencies were set symmetrical with respect to the spin tune in the $\Delta\nu_{\rm osc} = 0.005$ case.

The SF efficiency better than 99% should be achievable for the 3-4 times stronger AC dipole with $\Delta\nu_{\rm osc}$ kept at 0.02, sweep time $\tau_{\rm X}({\rm s})$ between $0.2 - 0.3{\rm s}$ and 28MHz+197MHz RF systems used.

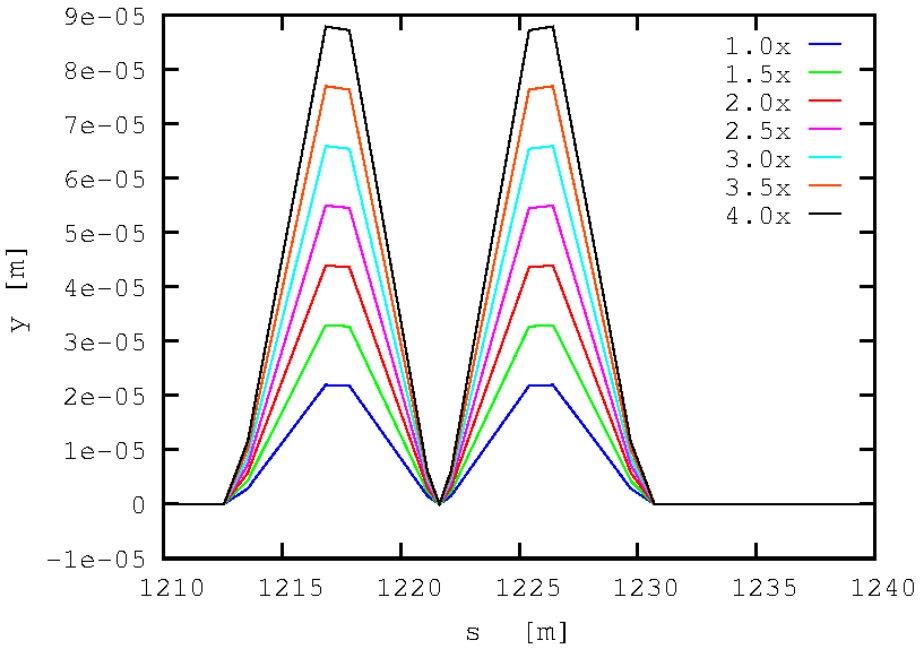

Figure 28: The maximum amplitude of the vertical ACD bumps is shown here for different strengths of the AC dipole at 255 GeV. $B_{osc}L$ was increased from 0.010 T.m up to 0.040 T.m.

Table 8: Comparing P_f/P_i after re-bucketing for different strengths of the Spin Flipper (the AC dipole part) and different sweep times $\tau_X(s)$ with $\Delta\nu_{osc} = 0.02$.

$B_{osc}L(T.m)$ \ $\tau_X(s)$	0.05	0.1	0.2	0.25	0.3	0.35
0.010 (nominal)	-	-	-	-84.0	-85.5	-85.2
0.015	-	-	-96.0	-96.1	-95.8	-95.2
0.020	-	-97.3	-97.5	-96.4	-	-
0.025	-96.0	-99.1	-98.0	-	-	-
0.030	-99.2	-99.4	-99.1	-	-98.6	-
0.035	-99.7	-99.6	-99.4	-	-99.2	-
0.040	-99.9	-99.8	-99.5	-	-99.3	-

Table 9: Comparing P_f/P_i after re-bucketing for different strengths of the Spin Flipper (the AC dipole part) and different sweep times $\tau_X(s)$ with $\Delta\nu_{osc} = 0.005$.

$B_{osc}L(T.m)$ / $\tau_X(s)$	0.025	0.05	0.075	0.1	0.15	0.2
0.010 (nominal)	-	-79.1	-85.8	-82.4	-	-60.5
0.015	-	-95.9	-	-95.5	-	-92.5
0.020	-	-97.5	-	95.2	-	-91.2
0.025	-98.8	-97.8	-	-95.5	-	-
0.030	-99.3	-98.9	-	-98.0	-	-

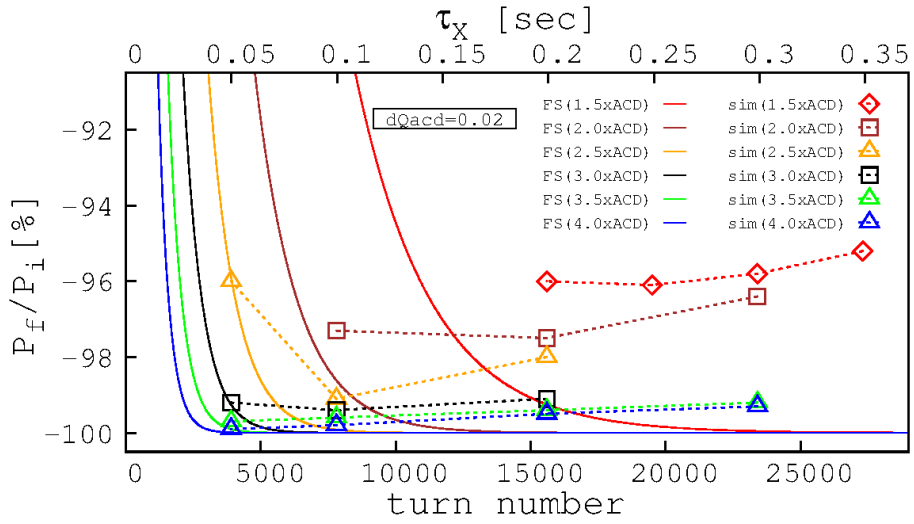

Figure 29: Spin Flip efficiency for different ACD strength. Simulations are done after re-bucketing at 255 GeV with $\Delta\nu_{\rm osc} = 0.02$ (namely $\nu_{\rm osc} = [0.48, 0.50]$ with $\nu_{\rm s} = 0.4962$). Froissart-Stora formula is plotted as well.

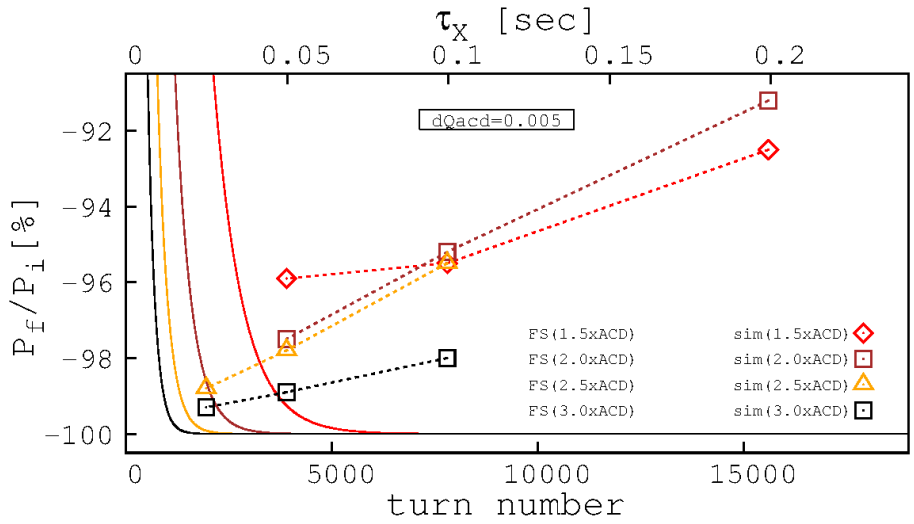

Figure 30: Spin Flip efficiency for different ACD strength. Simulations are done after re-bucketing at 255 GeV with $\Delta\nu_{\rm osc} = 0.005$. Froissart-Stora formula is plotted as well.

8 Conclusion

- The simulations of the sweep time scan and $\Delta D'$ scan at injection energy agree well with the FY17 APEX measurements. The results show that the optimal sweep time is 1 s for the driving tune range equal to 0.005. The simulations confirmed the SF efficiency dependence on $\Delta D'$ and that high $\Delta D'$ can cause the polarization loss during the spin flip due to the multiple resonance crossings.

- There is some agreement between the simulations and FY17 APEX measurements at 255 GeV. The sweep time scan 0.5 s measurement agrees with simulations within the (one sigma) error bars, but the 1.0 s measurement is about 3 sigma apart of the simulation results. Both simulations and measurements suggest that the optimal sweep time should be around 0.2 s for the driving range equal to 0.005.
  Multiple attempts were done to explain the 1 s measurement by introducing various errors into simulations. The fact of polarization drop at mirror resonance location at store, and not at injection, in the static spin tune scan suggests that there might be imperfection in the AC dipole orbit closure. The simulations confirmed that such an imbalance negatively affects the SF efficiency and might a reasonable explanation for the 1 s measurement.
  Note that the orbit at the Spin Flipper is not same (order of centimeters) at two energies due to the horizontal injection bump, and the different amplitudes of the DC and AC bumps. The store-to-store orbit jitter is only on order of tens of microns. It would be interesting to see if the different orbit settings at 255 GeV would help to improve the SF efficiency and/or eliminate the polarization drop at the mirror resonance location during the future APEX sessions.

- There is a good agreement between the measurements and simulations for the case of partially covered resonance at 255 GeV. This result emphasizes the importance of the spin resonance being fully covered by the driving tune range during the spin flip.

- Efforts were made to simulate the Spin Flip efficiency at 255 GeV at the nominal physics store settings after re-bucketing, using the 28MHz and 197MHz Rf system and the FY17 lattice. Different RF settings change the synchrotron frequency from 5 Hz to 50 Hz. The best Spin Flip efficiency for the FY17 APEX strength spin flipper was found to be only 86% even though $|\Delta D'|$ was minimized. The favorable settings for the driving tune range should be 0.02 (as oppose to 0.005) and the sweep time between $0.2 - 0.3$s if the future experiments are performed at these conditions.
  The simulations done with the stronger Spin Flipper show that the SF efficiency greater than 99% is achievable with the driving tune range being 0.02 and the sweep time between $0.2 - 0.3$s. The AC dipole was made up to 4x stronger in these simulations yielding the maximum amplitude of the ACD bump to be still only about $8.8 * 10^{-5}$m. The technical limitations on the AC dipole strength should be discussed.

- It is important to emphasize that the SF efficiency is less than 100% and does not agree with Froissart-Stora formula predictions for simulations which were done for high sweep times (3 s) with $|\Delta D'|$ being minimized down to the level that no multiple resonance crossings happen. Additionally the sweep time scan simulations with minimized $|\Delta D'|$ show the dependence of the SF efficiency on the RF settings, as it was shown for the 9MHz+197MHz versus 28MHz+197MHz case.

- The following observation based on the measured data and simulations can be done. The measured or simulated SF efficiency is never better than Froissart-Stora predictions. The deviations were mainly observed for larger sweep times. The simulations with anticipated parameters should be done prior to the future experiments, since the simulations were found to be explaining the measured SF efficiencies well. The optimal sweep time can be estimated based on the FS predictions and the measured SF efficiencies if needed, using a function which combines an exponential decay and linear increase as a function of sweep time.

- The Gγ scan at 255 GeV using the FY17 lattice showed a small dependence of the beam depolarization on Gγ. It would be interesting to perform additional scans before the upcoming FY22 polarized proton run.

References

[1] F. Méot *et al.*, RHIC Spin flipper, fast-sweep efficiency simulations BNL-114167-2017-IR, C-A/AP/589 (2017);

[2] M. Bai and T. Roser, Full Spin Flipping in the Presence of Full Siberian Snake, Phys. Rev. ST Accel. Beams 11, 091001 (2008).

[3] J. Kewisch *et al.*, Correction of the spin chromaticity in RHIC BNL-99842-2013-IR, C-A/AP/478 (2013);

[4] H. Huang, *et als.*, High Spin-Flip Efficiency at 255 GeV for Polarized Protons in a Ring With Two Full Siberian Snakes, Physical Review Letters 120, 264804 (2018).

[5] F. Méot, The ray-tracing code Zgoubi, NIM-A 427 (1999) 353-356 ; http://sourceforge.net/projects/zgoubi/

[6] F. Méot, *et als.*, On the effects of detector solenoids on n0 in RHIC and eRHIC, eRHIC Note 60, BNL (2018).

[7] NERSC computing, on web : http://www.nersc.gov/

[8] F. Méot, *et als.*, Re-visiting RHIC snakes - OPERA fields, $\vec{n}_0$ dance, Tech Note BNL C-A/AP/590 (9/22/2017).

[9] https://www.c-ad.bnl.gov/esfd/RMEM_12/Meetings/RHICStoreEnergyScan_Jan30_2012.pdf

A Gγ scan at 255 GeV

Most of simulations at 255 GeV were done at Gγ=487.5, which is slightly different than the FY17 APEX value 487.0. This small difference does not affect the SF efficiency for Spin Flip, when the oscillator frequency range well covers the resonance.

This section compares simulations using FY17 lattice with $\nu_y = 0.684$ at three different Gγ, 487.0, 487.5 and 488.0. This was partially motivated by previous RHIC store energy studies [9].

The initial polarization before the Spin Flip is less than +1 at 255 GeV, as mentioned in 4.1. The multiparticle simulations over 2000 turns with Spin Flipper turned off were done to examine the beam depolarization in more details. Fig. 31 shows a behavior of the average vertical spin coordinate for three different Gγ. Plot suggests that the beam depolarizes at Gγ = 488.0 slightly less than at 487.0 or 487.5.

The stable spin direction for particles with non-zero vertical emittance is not vertical. Fig. 32 shows how the averaged vertical spin component of particles with different vertical emittance depends on Gγ.

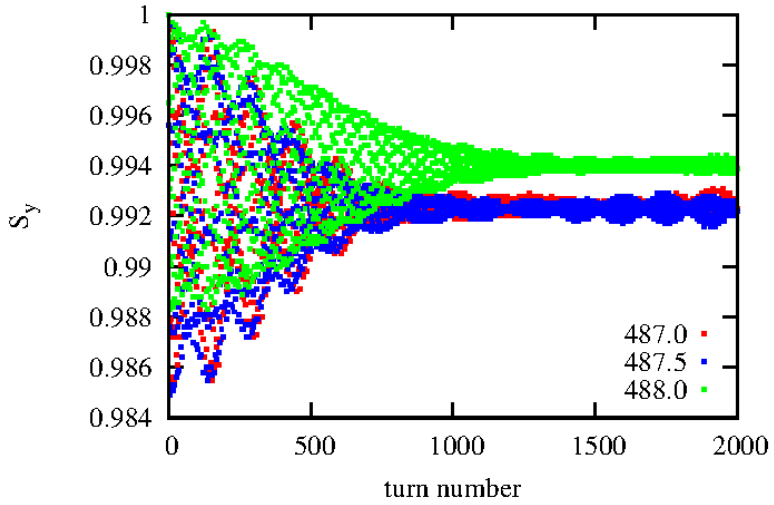

Figure 31: Average vertical spin coordinate of the particle bunch shows the beam depolarization at 255 GeV (for Gγ equal to 487.0, 487.5 and 488.0.). The simulations were setup for FY17 APEX conditions, with Spin Flipper turned off.

The width of the Spin Flip can be defined as a range of the oscillator frequencies during which particle's vertical spin component is equal 0, given that the Spin Flip is set such that all particles begin with S_y = +1 and finish with $S_y \approx$ -1. Fig. 33 shows tracking of the vertical spin component of 40 random particles during a Spin Flip with τ_X=0.2 s, $\Delta\nu_{osc}$ = 0.005 and $\Delta D'$ = 0.12mrad. The spin flip is "wider" for Gγ = 487.0 than Gγ = 488.0 as depicted by the arrows.

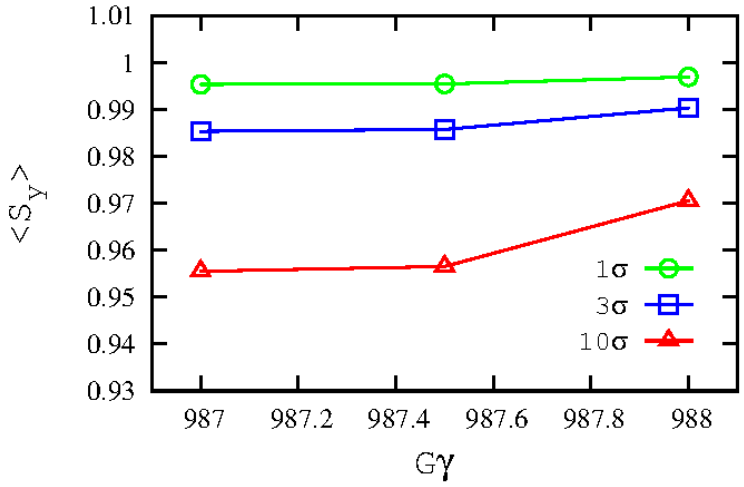

Figure 32: Average vertical spin coordinate over 2000 turns for particles with different vertical emittance (1σ, 3σ and 10σ with $\beta\gamma\varepsilon_{\mathrm{y,RMS}}$=2.7 μm) at 255 GeV (for Gγ equal to 487.0, 487.5 and 488.0.). The simulations were setup for FY17 APEX conditions, with Spin Flipper turned off.

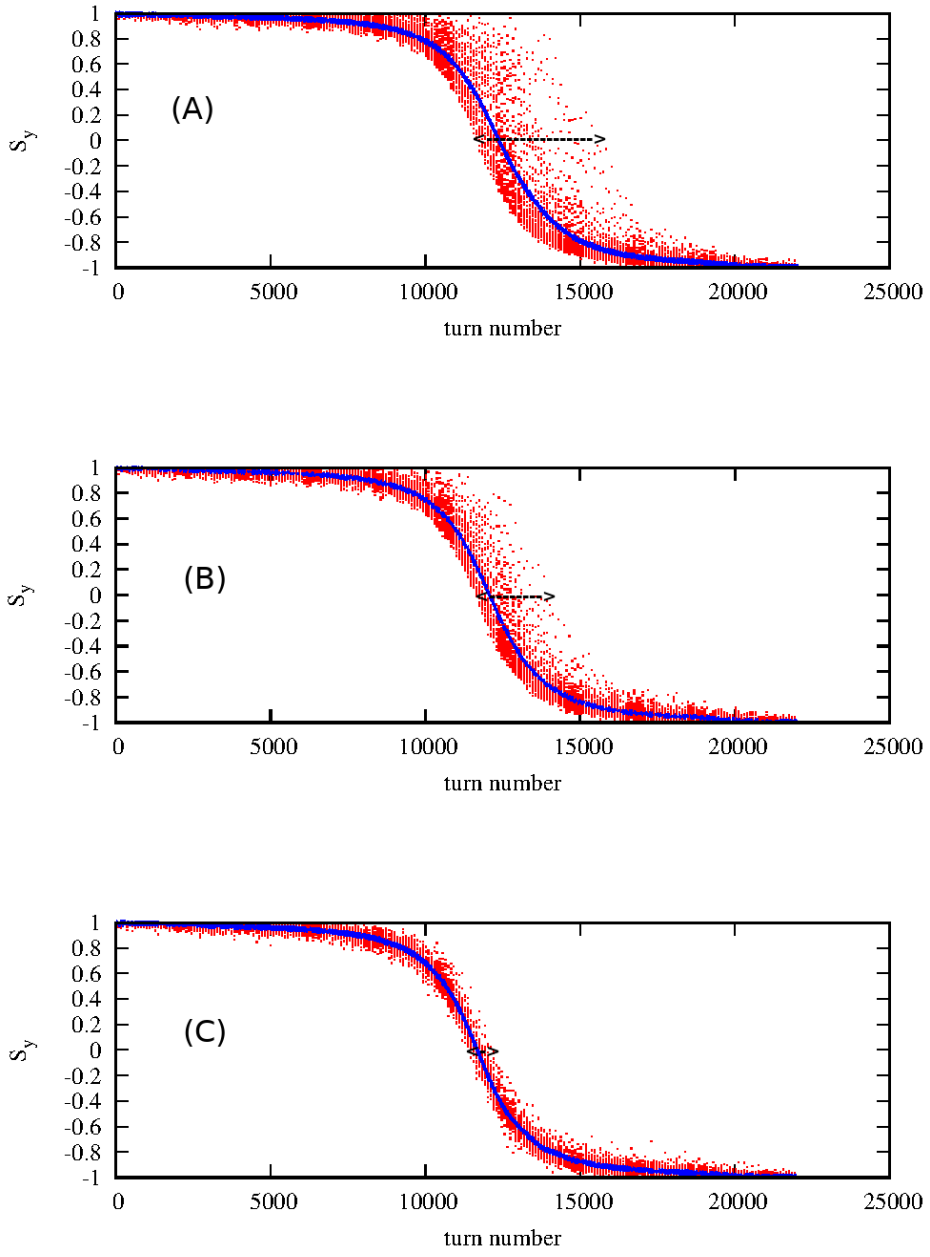

Figure 33: Simulations of Spin Flip at 255 GeV using FY17 lattice with τ_X=0.2 s and $\Delta D' = 0.12$ mrad for three slightly different values of $G\gamma$: (A) $G\gamma = 487.0$, (B) $G\gamma = 487.5$ and (C) $G\gamma = 488.0$. The width of the Spin Flip is somewhat dependent on $G\gamma$. Red - vertical spin component of individual particles; Blue - average vertical spin component of the 10^3 particles.

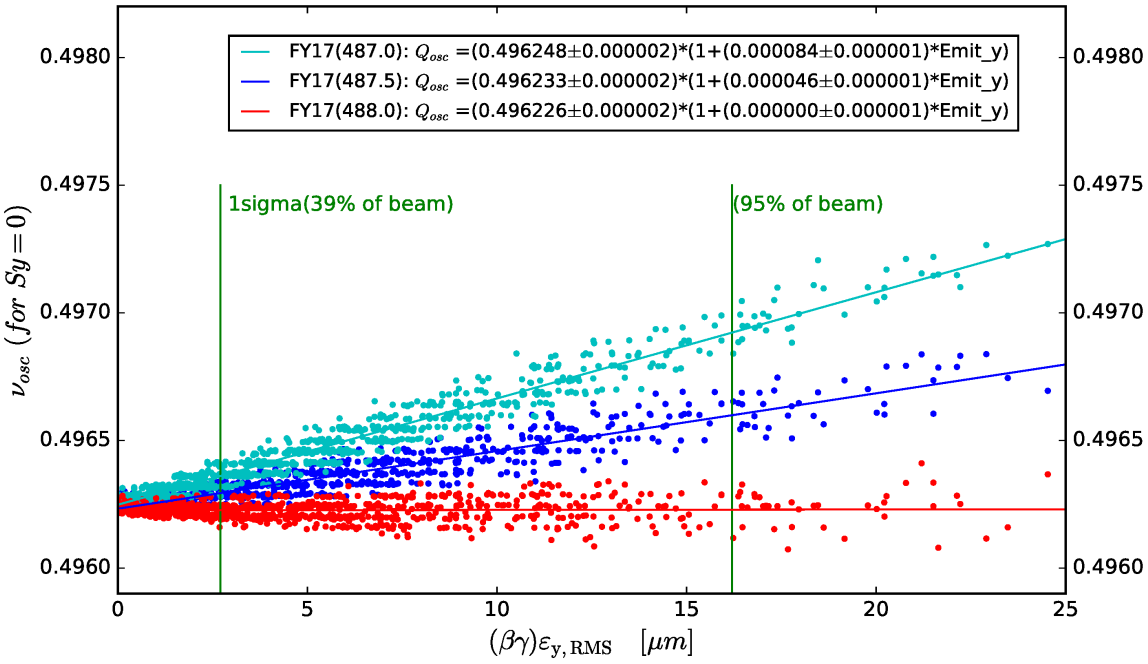

Figure 34: Simulations show that particles with bigger vertical emmitance go through the spin flip at higher oscillator frequencies at Gγ = 487.0. There is no such dependence at Gγ = 488.0. The frequency of the oscillator at which the particle's vertical spin component crosses zero for the first time during the Spin Flip is plotted here versus the particle's normalized emmitance (its vertical invariant). Simulations were done at 255 GeV for three different value of Gγ, with $\Delta \mathrm{D}' = 0.1\,\mathrm{mrad}$, $\Delta\nu_{\mathrm{osc}} = 0.005$ and 0.2 s sweep time using FY17 lattice with $\nu_{\mathrm{y}} = 0.684$.